Pterosaur remains from uppermost Lower Cretaceous (Albian) of China, with comments on the femoral osteological correlates for thigh muscles

Junyi Song [a, b], Shunxing Jiang [a, *], Xiaolin Wang [a, b]

[a] *Key Laboratory of Vertebrate Evolution and Human Origins, Institute of Vertebrate Paleontology and Paleoanthropology, Chinese Academy of Sciences (CAS), Beijing, 100044, China*
[b] *College of Earth and Planetary Sciences, University of Chinese Academy of Sciences, Beijing, 100049, China*

ABSTRACT

Pterosaurs, an extinct group that ruled Mesozoic skies, flourished during the Cretaceous. Knowledge about their radiation largely comes from several Lagerstätten, especially in China and Brazil. Despite their abundance and diversity in other continents during the latest Early Cretaceous, pterosaurs from East Asia in this period are extremely rare, rendering their evolutionary history still unexplored. Here we redescribe pterosaur remains from the Albian Doushan Formation of Laiyang, Shandong Province, China, to refine such gap. The most completely preserved element, a femur, can be assigned to the Azhdarchoidea, a clade achieving global distribution by the end of the Early Cretaceous, based on combination of derived and plesiomorphic characters including the triangular and anteriorly curved 'greater trochanter', a deep 'intertrochanteric fossa' with a pneumatic foramen, presence of a bulbous ridge and a pulley-like lateral condyle. Moreover, osteological correlates for thigh muscles on the femur are identified here using the Extant Phylogenetic Bracket method. The general pattern of these osteological correlates is conservative when compared with other basal ornithodirans. The pterosaurian 'greater trochanter' is not homologous to the lesser trochanter in other archosaurs as previously suggested. M. femorotibialis internus is subdivided into two parts in some pterosaurs, probably representing a derived trait.

© 2023 Elsevier Ltd. All rights reserved.

1. Introduction

Pterosaurs are an extinct group of reptiles that were the first vertebrates to evolve powered flight (Wellnhofer, 1991). The fragile architecture of pterosaur skeletons makes them extremely rare in terrestrial strata (Barrett et al., 2008). In China, pterosaurs are well-represented from a few sites or strata, e.g., the Yanliao and Jehol biotas in northeastern China (Wang et al., 2005; Xu et al., 2016) and Tugulu Group in Xinjiang (Young, 1964, 1973; Wang et al., 2014a). Such distribution means that our knowledge of East Asian pterosaurs has been restricted to scattered time slices, e.g., late Middle Jurassic—early Late Jurassic (Yanliao Biota) and Barremian—Aptian (Jehol Biota). Few pterosaurian remains have been found from other time slices in China, and most of these are fragmentary and

awaiting further study. For example, pterosaurs diversified and were globally widespread during Albian—Cenomanian with an extensive fossil record around the world, especially in South America and Europe (Barrett et al., 2008). However, pterosaurs in East Asia during this period are poorly documented.

Young (1958, 1964) briefly reported pterosaur remains from the Albian Doushan Formation, Qingshan Group of Laiyang, Shandong Province, which was dated ~107 Ma (Wang et al., 2022). They are the first described pterosaurs and among the few, if not the only one reported from the uppermost Lower Cretaceous in China providing uncertain ages of some other pterosaur remains. Young (1964) assigned these postcranial elements to *Dsungaripterus* and other researchers considered them to be Dsungaripteridae indet. (Unwin and Heinrich, 1999; Barrett et al., 2008). Upchurch et al. (2015) mentioned that they cannot be referred to Dsungaripteridae, yet without referring them to another clade. Considering the controversy on the affinities of this material and the scarcity of pterosaur remains from the Albian of East Asia, here we provide a detailed description and taxonomic assignment of these remains.

The current work finds that little evidence supports the original referral to Dsungaripteridae.

In addition, the excellently preserved femur provides an opportunity to identify the osteological correlates of pterosaurian thigh muscles on this bone. Thigh muscles and their osteological correlates have been extensively investigated in extinct archosaurs within the frame of evolution and biomechanics. They have been utilized as characters in phylogenetic analyses (Gauthier, 1986; Novas, 1996; Nesbitt, 2011) and ontogeny (Nesbitt et al., 2009; Griffin and Nesbitt, 2016; Griffin, 2018) or as proxies for postures and locomotory capabilities (Allen et al., 2021) in different fossil groups. Despite the extensive interest in pterosaurian locomotion, e.g., stance and flying postures of pterosaurs (Padian, 1983; Bennett, 1997; Griffin et al., 2022), thigh muscle reconstructions, which have been proved important for inferring these characters, are relatively scarce (Fastnacht, 2005; Costa et al., 2013; Frigot, 2018). Furthermore, most previous attempts do not apply an Extant Phylogenetic Bracket (EPB sensu Witmer, 1995) or provide detailed osteological correlates, which makes comparisons among different taxa difficult. Considering the tremendous diversity of limb ratios in pterosaurs, diversified locomotion modes among groups are expected (Bennett, 1997). In that sense, variation of osteological correlates for muscles could be an indication of these differences. Here we attempt to provide detailed illustration of osteological correlates of thigh muscles, and intend to shed light on the evolution of pterosaurian femora.

Institutional Abbreviations—**AOD**, Australian Age of Dinosaurs Natural History Museum, Winton, Australia; **BSP**, Bayerische Staatssammlung für Paläontologie und historische Geologie, Munich, Germany; **IVPP**, Institute of Vertebrate Paleontology and Paleoanthropology, Beijing, China; **MGUAN-PA**, Museu Geológico Universidade Agostinho Neto—Projecto PaleoAngola; **MTM**, Magyar Természettudományi Múzeum (Hungarian Natural History Museum), Budapest, Hungary; **NHMUK**, Natural History Museum London, UK; **NMV**, Melbourne Museum, Museums Victoria, Melbourne, Australia; **PMOL**, Paleontological Museum of Liaoning, Shenyang, China; **SDUST**, Shandong University of Science and Technology, Qingdao, China; **SMNK**, Staatliches Museum für Naturkunde Karlsruhe, Karlsruhe, Germany; **TMP**, Royal Tyrrell Museum of Palaeontology, Drumheller, Canada; **YPM**, Yale Peabody Museum, New Heaven, Connecticut, USA; **ZIN PH**, Palaeoherpetological collection, Zoological Institute, Russian Academy of Sciences, Saint Petersburg, Russia.

2. Materials and methods

The specimens described here (IVPP V 746, IVPP V 747, and IVPP V 755) were collected in Laiyang, Shandong Province (Fig. 1A, B), from Doushan Formation, the same horizon as numerous skeletons of *Psittacosaurus sinensis* were found (Fig. 1C; "the upper part of Chinshan Beds in dark red clay" according to Young, 1958; Hu et al., 2001). The material comprises a right femur (Figs. 2–4) and a proximal portion of a second wing phalanx (Fig. 5A, B) (IVPP V 746); a purported right tibiotarsus (Fig. 5C-E) and a proximal portion of a first wing phalanx (Fig. 5F-H) (IVPP V 747); and a purported left tibiotarsus (Fig. 5I) (IVPP V 755). It should be mentioned that we cannot determine what the specimen number means, i.e., whether it refers to a single locality or a single individual, due to a lack of excavation records. Thus specimens under the same number are here treated as different individuals. The anatomical terminology follows that of Bennett (2001a). When referring to the longitudinal axis, 'proximal' and 'distal' are used instead of 'dorsal' and 'ventral' to avoid confusion. The bone dimensions are measured with a 150 mm digital caliper with 0.01 mm resolution. For comparison, specimens of *Sinopterus dongi*, *Dsungaripterus weii*, *Noripterus*

complicidens, and *Hamipterus tianshanensis* housed in IVPP are examined by first-hand observation. Single quotation marks of greater trochanter and intertrochanteric fossa are used to avoid confusion of homology between the structure in pterosaurs and that in other groups (i.e., dinosaurs in the former case and lizards in the latter case) with the same name.

The phylogenetic backbone used in this article follows Ezcurra et al. (2020) (Archosauria); Pêgas et al. (2021) and Xu et al. (2022) (Pterosauria ingroup). EPB is utilized to reconstruct pterosaurian thigh muscles based on their osteological correlates (Witmer, 1995). EPB requires bracketing extant outgroups of extinct taxa for comparison. Level I, II, and III inferences refer to the presence of muscle of interest and its osteological correlate in both, one and none of the bracketing extant outgroups respectively. Level inferences with a quotation mark, i.e., that possess the muscle of interest though without an osteological correlate, are treated the same as level inferences without it. As we subscribe to the ornithodiran hypothesis, with Lagerpetidae as a member of Pterosauromorpha or Dinosauromorpha (Ezcurra et al., 2020), the extant outgroups are crocodiles and birds. Information about muscles and their osteological correlates in extant and extinct organisms is mostly collected from the literature (e.g., Romer, 1923; George and Berger, 1966; Langer, 2003). Muscular homology and nomenclature follows Rowe (1986) and Hutchinson (2001a).

3. Results

3.1. Description

Specimen IVPP V 746 consists of a right femur (Fig. 2). The well-developed muscle scars, and smooth texture of the bone surface indicate that it belongs to a mature individual (Bennett, 1993). The femur is broken into three fragments, though little compaction can be detected. It is straight in anterior view and mildly bowed anteriorly in lateral view. The shaft expands laterally at the base of the 'greater trochanter' and then decreases in diameter distally. It remains a constant diameter and an oval cross-section with the long axis in mediolateral direction for half the length of the shaft (Fig. 2). The distal shaft gradually expands and has a D-shaped cross-section with a flattened posterior surface. The cortical bone is quite thin and the R/t value sensu Currey and Alexander, 1985 is estimated as 5.6 (long axis) ~8.9 (short axis) at the broken area of the proximal fragment, typically seen in pterosaurs except for dsungaripterids (3.3–3.9 in the femur of *Noripterus complicidens*; Fastnacht, 2005).

The proximal end is characterized by the femoral head and a prominent 'greater trochanter'. A constricted neck connects the femoral head to the shaft and is oriented proximomedially with an angle of 135° relative to the diaphysis (Fig. 3A, G), contrasting with the ~160° angle of pteranodontoids (Unwin, 2003). The head is bulbous and rounded as in most pterosaurs, unlike the more oval head of *Dsungaripterus weii* and *No. complicidens*. It expands more anteromedially than posterolaterally relative to the neck, as commonly seen in pterodactyloids (Kellner and Tomida, 2000; Bennett, 2001a; Andres and Langston, 2021). It is broken at the posteromedial side and the existence of a notch, i.e., fovea capitis (Tsai and Holliday, 2015), cannot be determined. Distal to this breakage the posterior neck surface is rather striated, indicating acetabular ligament insertion (Fig. 3D, J). The femoral neck is slender and elongated, the length of which measured about 0.88 the diameter of the head (Table 1; neck length is measured from the head-neck junction to the base of the anterior flange between the neck and greater trochanter). The neck has an oval cross section with the ratio of maximum and minimum diameter approximately 1.44. It is connected to the 'greater trochanter' by a flange anteriorly
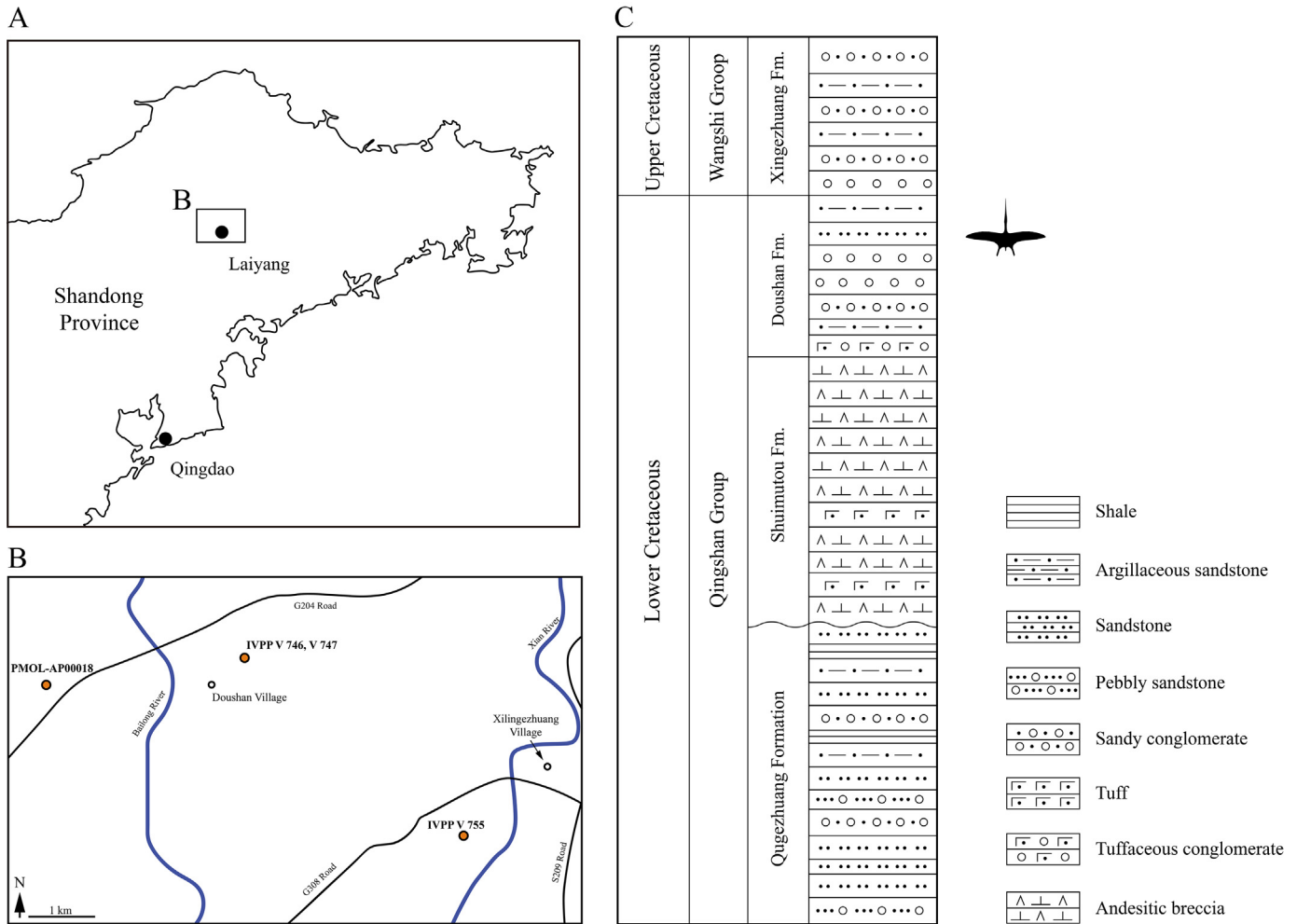
Fig. 1. A, **B**, Maps showing localities of IVPP V 746, IVPP V 747, IVPP V 755 and PMOL-AP00018 according to Young (1958) and Zhou (2010); **C**, Stratigraphic column of Qingshan Group in Laiyang, showing the fossil beds of Doushan Formation (modified from Hu et al., 2001). The silhouette is sourced from https://www.phylopic.org/.

and is confluent with the shaft posteriorly, bordering the 'inter-trochanteric fossa' inside which a large pneumatic foramen rests (Fig. 3E, F). In proximal view, a small oval neurovascular foramen is present on the lateral portion of the anterior flange (Fig. 3E, F). The 'greater trochanter' is elevated and has a broad base with a triangular outline in anterior view. Though the anterior portion is broken, the curvature indicates that the 'greater trochanter' is anteriorly curved. A well-excavated and proximodistally elongated lateral fossa is present on the lateral surface of the 'greater trochanter' (Fig. 3B, H). It is bordered distally by a rugose expanded area, yet the exact morphology cannot be determined due to crushing. This lateral fossa is commonly reported in pterosaurs (Fastnacht, 2005; McLain and Bakker, 2017; Bertozzo et al., 2021; Augustin et al., 2021a) and probably serves as the insertion site for M. pubo-ischio-femoralis externus (PIFE) complex. On the anterior surface of the proximal shaft, two succeeding tubercles are present distal to the 'greater trochanter' (Fig. 3A, G). The proximal one is more prominent and elongated, corresponding to the lesser trochanter. The distal one is slightly oblique and has not been reported in other pterosaurs. This protuberance, here termed accessory tubercle, is probably autapomorphic for this femur. The lesser trochanter corresponds to insertion for M. iliofemoralis (IF), whereas the accessory tubercle corresponds to insertion for M. puboischiofemoralis internus 2 (PIFI2; Fig. 2F). A jagged anterior ridge, the linea intermuscularis cranialis (LIA), originates from the proximal base of the proximal tubercle. This is also seen in *D. weii*, *No. complicidens*, the Hungary dsungaripteroid SHN.013 (Bertozzo et al., 2021) and *Hamipterus tianshanensis* but is different from an indeterminate pteranodontid (ZIN PH 66/43), whose LIA extends to the neck (Fig. 6G; Averianov and Arkhangelsky, 2020). The LIA curves medially and extends further down the shaft. It becomes nearly invisible at the distal extremity of the proximal fragment.

Posteriorly, a bulbous ridge is present distal to the 'greater trochanter' (Fig. 3D, J). It is proximally wide and extends distally with a long 'tail'. This bulbous ridge is prominent in azhdarchoids (Manzig et al., 2014; Zhang et al., 2019; Andres and Langston, 2021), serving as the insertion site for M. ischiotrochantericus (ISTR; Fig. 2E). A shelf-like bone connects the distal end of the bulbous ridge and the base of the lateral fossa. The fourth trochanter for M. caudofemoralis longus (CFL) insertion ("internal trochanter" in Kellner and Tomida, 2000; Bennett, 2001a) lies medial to the bulbous ridge. It is an elongated and curved ridge, bounding a medial depression, as in many pterosaurs, e.g., *Azhdarcho lancicollis* (ZIN PH 16/44) and *Anhanguera piscator* (Kellner and Tomida, 2000; Averianov, 2010). On the medial surface, a longitudinally elongated muscle scar for M. pubo-ischio-femoralis internus 1 (PIFI1; Fig. 3C, I) is visible. Anterior to the PIFI1 insertion is a proximally opening neurovascular foramen. A small rugose raised area is present distal to the PIFI1 insertion on the distal extremity of the proximal fragment.
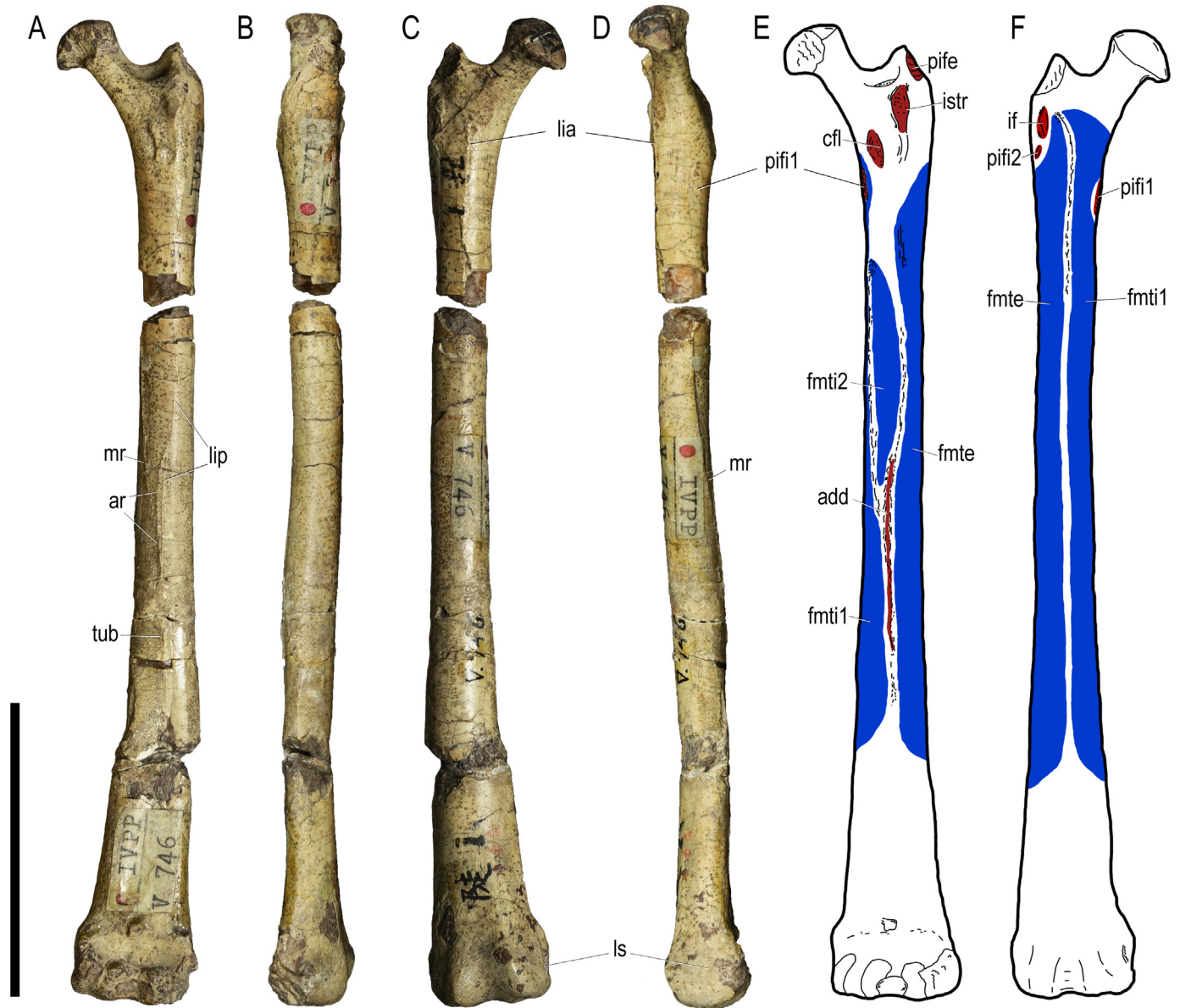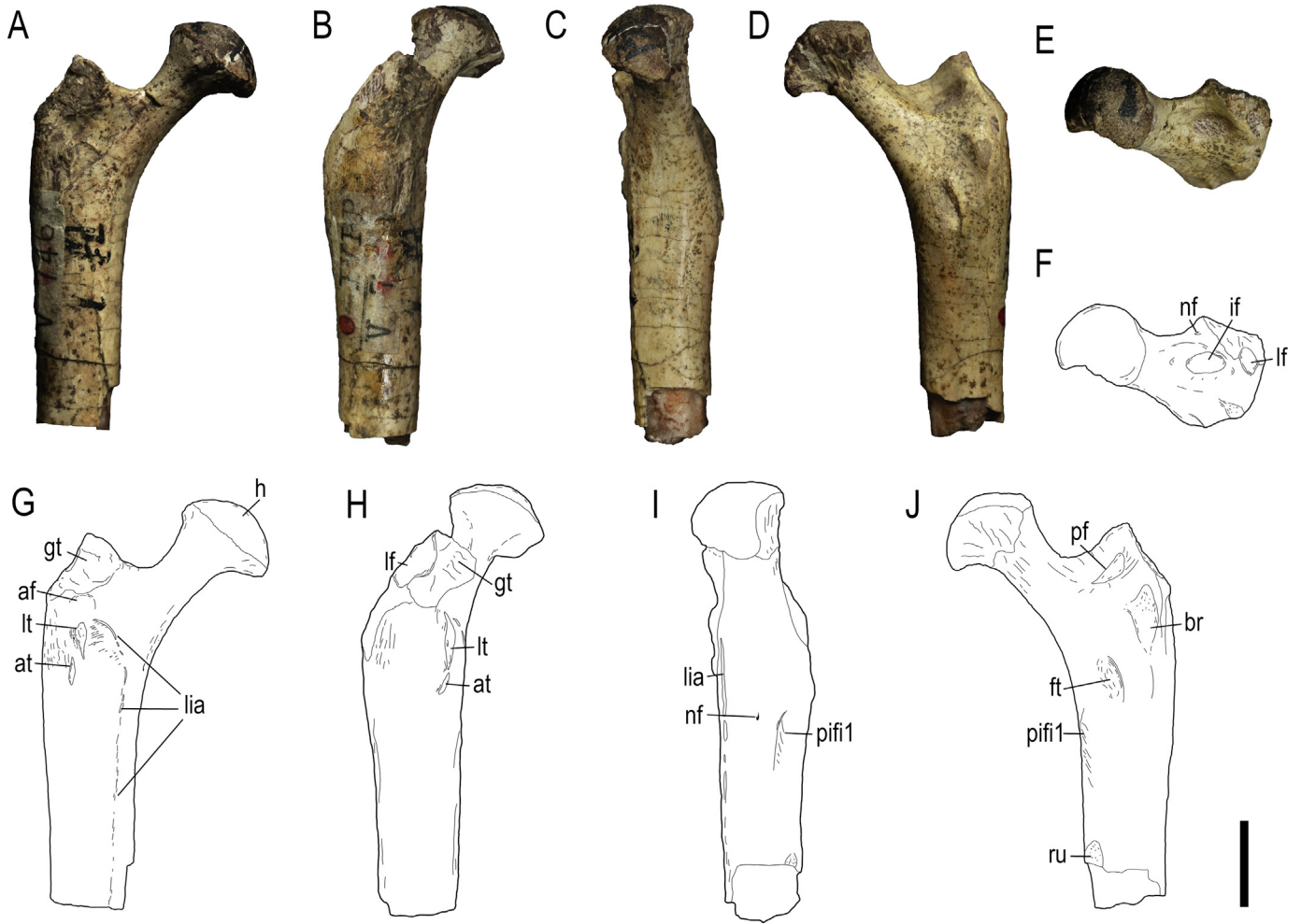
Fig. 2. The right femur of IVPP V 746. Photographs of the femur in **A**, posterior; **B**, lateral; **C**, anterior; **D**, medial views. Line drawings of the femur showing muscle attachments in **E**, posterior; **F**, anterior views. Origins are indicated by blue and insertions are indicated by red. **Abbreviations**: add, insertion for Mm. adductor femorales 1 et 2; ar, adductor ridge; cfl, insertion for M. caudofemoralis longus; fmte, origin of M. femorotibialis externus; fmti1, origin of the anterior head of M. femorotibialis internus; fmti2, origin of the posterior head of M. femorotibialis internus; if, insertion for M. iliofemoralis; istr, insertion for M. ischiotrochantericus; lia, linea intermuscularis cranialis (anterior ridge); lip, linea intermuscularis caudalis; ls, ligament scar; mr, medial ridge; pife, insertion for M. puboischiofemoralis externus complex; pifi1, insertion for M. puboischiofemoralis internus 1; pifi2, insertion for M. puboischiofemoralis internus 2; tub, prominent tuberosity. Scale bar equals 50 mm.

At the proximal extremity of the middle fragment, a medial ridge extends posterodistally and joins two posterior ridges. This medial ridge might be continuous with the small rugose and raised area on the proximal fragment. This medial ridge is also present in *No. complicidens*, *Quetzalcoatlus* cf. *northropi*, *Quetzalcoatlus lawsoni* (Andres and Langston, 2021) and *Pteranodon* sp. (YPM 1175, 2546; photos available at the website of Yale Peabody Museum, https://peabody.yale.edu/explore/collections). Of the two posterior ridges, the lateral ridge originates from the proximal extremity of the middle fragment and is quite shallow, representing the linea intermuscularis caudalis (LIP; Fig. 2A, E), whereas the medial ridge is more prominent and has a more distal origin, representing the adductor ridge (AR; Fig. 2A, E). After extending parallel along the shaft for 23 mm, the ridges converge and further form a prominent

tuberosity ('fourth trochanter' of Kellner and Tomida, 2000; Bennett, 2001a; Andres and Langston, 2021). The ridges then rapidly become disappear before reaching the distal end. The area between LIA and AR is mediolaterally narrow, providing the insertion for Mm. adductor femorales 1 et 2 (ADD; Fig. 2A, E).

On the posterior surface of the distal fragment, a tuberosity is present on the posterior surface proximal to the popliteal fossa, which is not seen in any other pterosaurs to our knowledge (Fig. 4A, B). It cannot be referred to as attachment for any muscle or ligament. The tuberosity is peculiarly smooth and elevated abruptly, significantly different from what might be expected in tendon attachments (Benjamin et al., 2002), so it is tentatively considered here as a pathology. A shallow ridge passes the peculiar tuberosity and forms the proximal margin of the popliteal fossa. It is further
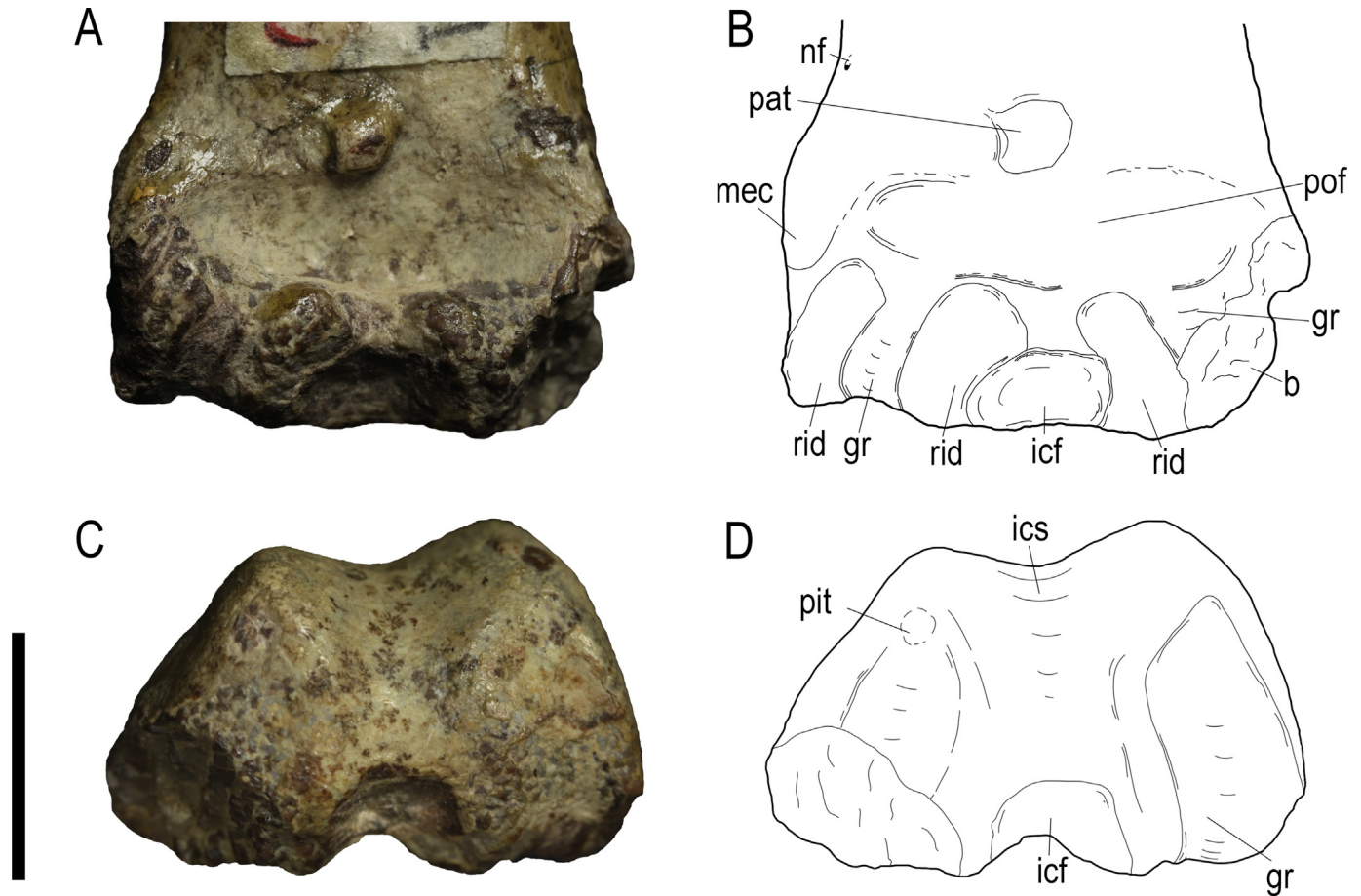
Fig. 3. Proximal fragment of the right femur, IVPP V 746. Photographs of the proximal fragment in **A**, anterior; **B**, lateral; **C**, medial; **D**, posterior; and **E**, proximal views. Line drawings of the proximal fragment in **F**, proximal; **G**, anterior; **H**, lateral; **I**, medial; and **J**, posterior views. **Abbreviations**: af, 'anterior fossa'; at, accessory tubercle; br, bulbous ridge; ft, fourth trochanter; gt, 'greater trochanter' (distinct process); h, femoral head; lia, linea intermuscularis cranialis (anterior ridge); lf, lateral fossa; lt, 'lesser trochanter'; nf, neurovascular foramen; pf, pneumatic foramen; pifi1, insertion for M. puboischiofemoralis 1; ru, rugose raised area. Scale bar equals 10 mm.

bounded distally by the posteriorly expanded condyles. Several small foramina are present in the fossa. The popliteal fossa serves as the origin for digital flexor muscles (Bennett, 2001a). The distal end is only mildly expanded relative to the shaft. In distal view, it has a trapezoidal outline, composed of the two condyles and a large and deep intercondylar fossa posteriorly. The lateral condyle deviates more from the parasagittal plane than the medial one (Fig. 4C, D), as in other pterosaurs except for *Az. lancicollis* (ZIN PH 20/44), whose distal ends are nearly symmetrical (Averianov, 2010). The condyles are separated by a shallow and wide intercondylar sulcus that narrows onto the distal surface and forms the anterior margin of the intercondylar fossa. It doesn't deepen distally to form a transverse ridge like that of *Az. lancicollis* (Averianov, 2010). The intercondylar fossa is sub-rectangular with a long axis oriented mediolaterally. The medial condyle is pulley-like, with a groove extending from the posterior to the distal surfaces and two ridges surrounding the groove (Fig. 4A, B). This groove could fit into the posteromedial prominence on the articular surface of the tibiotarsus. Although the lateral condyle is damaged, a groove can also be detected and is bounded medially by a ridge, hence it is also pulley-like. A round pit is present anterior to this groove on the distal surface of the lateral condyle (Fig. 4C, D).

Proximally, the two ridges surrounding the intercondylar fossa are swollen, with the medial one more bulbous than the lateral

condyle. In medial view, the medial epicondyle is moderately developed and continuous with the posterior corner of the medial condyle. An oval neurovascular foramen opening proximally is present proximal to this tubercle. A longitudinal scar is visible on the medial aspect of the medial condyle, probably for the attachment of collateral ligament as in birds (Fig. 2C, D; McGowan, 1979; Baumel and Witmer, 1993). The lateral portion of the lateral condyle has been broken away and no information can be inferred.

IVPP V 746 also includes a proximal end of a second wing phalanx (Fig. 5A, B). It is dorsoventrally flattened but with no pneumatic foramen found in *Pteranodon* sp. (Bennett, 2001a). One side of the shaft has a shallow and broad median groove, suggesting that this is the ventral side. The articular surface is concave and teardrop-shaped with the ratio of width to depth about 2 (Fig. 5A; Table 1), unlike the subcircular and weakly concave cotyle of *Pteranodon* sp. (Bennett, 2001a). The posterior expansion of the articular surface is more prominent ventrally. A prominent tubercle is present anterior to the articular surface, as in other pterosaurs (Andres and Langston, 2021). In dorsoventral view, the anterior margin of the proximal end has a slightly convex profile, whereas the posterior margin has a considerably concave profile. The bone surface around the articular surface is rugose and serves as attachment for a ligament. The gross morphology of the proximal end suggests that this specimen represents a right second wing

Fig. 4. Distal fragment of the right femur, IVPP V 746. **A**, Photograph, and **B**, line drawing of the distal fragment in posterior view. **C**, Photograph, and **D**, line drawing of the distal fragment in distal view. **Abbreviations**: b, breakage; gr, groove; icf, intercondylar fossa; ics, intercondylar sulcus; mec, medial epicondyle; nf, neurovascular foramen; pat, pathology; pit, round pit; pof, popliteal fossa; rid, ridge. Scale bar equals 10 mm.

phalanx, as the third or fourth wing phalanges have a more rounded proximal end, without a prominent anterior tubercle (Andres and Langston, 2021).

IVPP V 747 includes a proximal portion of a right first wing phalanx (Fig. 5F–H). In dorsal view, the proximal end is anteroposteriorly expanded affected by the anterior and posterior expansion. The former is blunt and rugose. The latter is sharp and develops into a process (Fig. 5F). The extensor tendon process (ETD) has been completely fused without a visible suture, indicating this specimen represents an individual that at least reaches OS5 of Kellner (2015) and is significantly smaller than that represented by the Laiyang femur (V 746). The ETD is sub-rectangular and projects proximally and anteroventrally. No proximal groove sensu Frey and Martill (1998) can be identified. In proximal view, two cotyles are present as in other pterosaurs (Fig. 5D). The ventral cotyle extends anteroproximally to posterodistally, and is deepest at its posterodistal portion due to the proximal projection of its ventral boundary. The dorsal cotyle is shallow and crescentic. It extends anteroposteriorly to form a ~70° angle with the ventral cotyle in ventral view. Its dorsal boundary is swollen at its anterior end and slopes posteriorly, whereas its ventral boundary is almost horizontal. A pneumatic foramen present at the anterior side of the dorsal cotyle in *Pteranodon* sp. is not found (Bennett, 2001a). On the ventral surface, a large oval pneumatic foramen is present in a depression between these two cotyles (Fig. 5B), a common condition in ornithocheiroids (Andres, 2021) except for dsungaripterids (Young, 1964; Augustin et al., 2021b). The pneumatic foramen

nearly occupies the whole depression. The shaft is quite straight. The cross section of the proximal shaft is oval with an anteroposterior long axis, whereas that of the distal fragment is subtriangular with the dorsal surface flattened.

IVPP V 747 also includes a proximal shaft of a probable right tibiotarsus, though without trace of the fibula (Fig. 5C–E). The shaft diameter decreases rapidly. The cross-section is triangular proximally and oval distally (Fig. 5D, E). The surface of the longest side of the triangular in the proximal section represents the anterolateral face, while that of the shortest side represents the medial side. A longitudinal rugose scar is present on the proximomedial shaft, as in *Pteranodon* sp. (Bennett, 2001a).

IVPP V 755 is a left tibiotarsus (Fig. 5I). The proximal part is less well preserved than IVPP V 747. A longitudinal ridge is present posteromedially on the distal shaft. Note that the shaft diameter is relatively constant for distal one-third of the preserved length (the portion distal to the plaster most probably doesn't belong to it). Further information cannot be determined.

3.2. Osteological correlates for thigh muscles on the femur

3.2.1. The 'greater trochanter' and 'lesser trochanter'

The lateral aspect of the proximal femur in pterosaurs shows some variation. In basal pterosaurs, e.g., *Campylognathoides liasicus* and *Dimorphodon macronyx*, this area is expanded and rugose (Fig. 6D; Padian, 2008; Sangster, 2021). In basal monofenestratans, e.g., *Wukongopterus lii* (IVPP V 15113; Fig. 6E) and *Kunpengopterus*
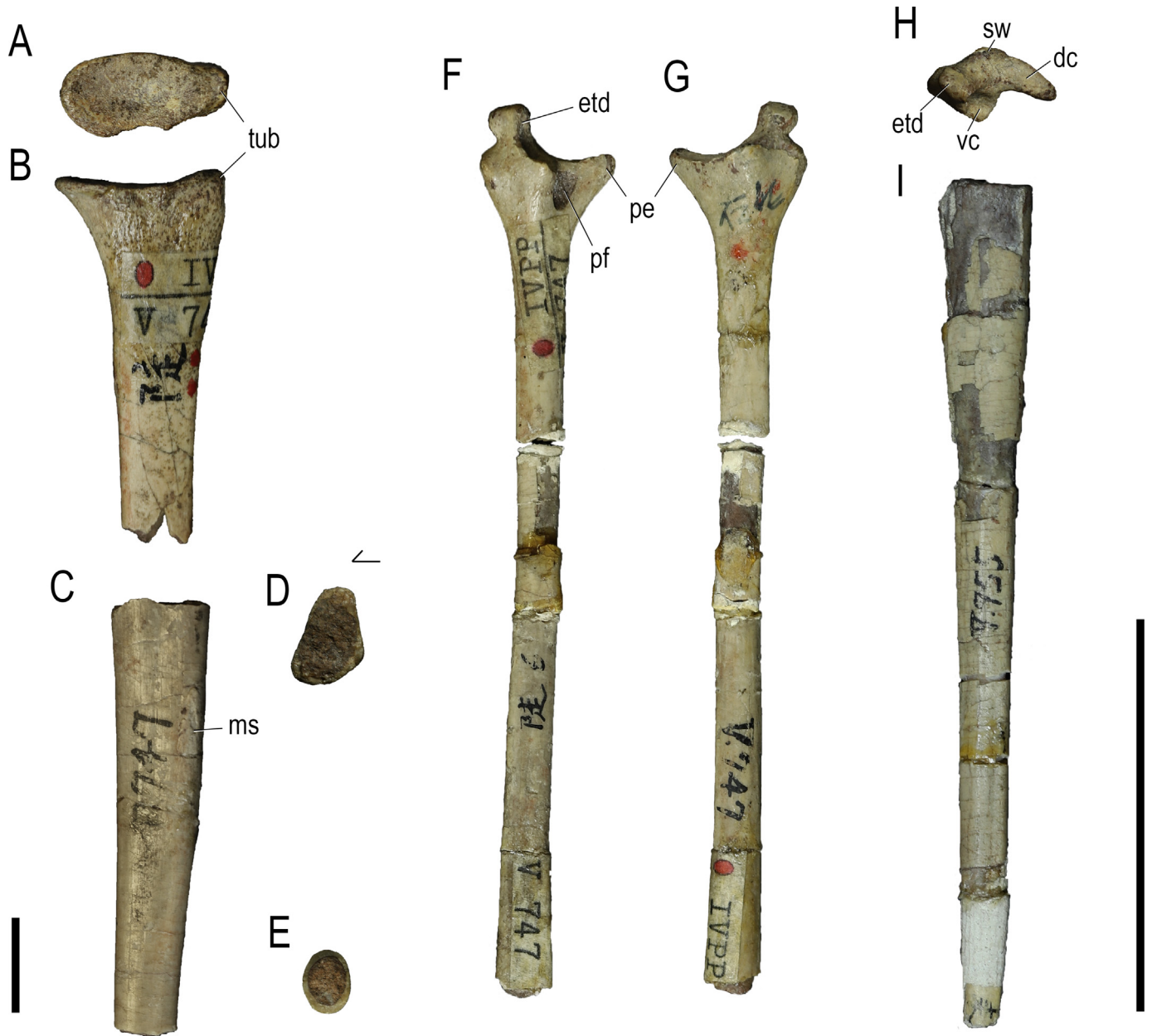
Fig. 5. A right second wing phalanx, IVPP V 746 in **A**, proximal; and **B**, dorsal views; a right tibiotarsus, IVPP V 747 in **C**, anterior; **D**, proximal; and **E**, distal views; a right first wing phalanx, IVPP V 747 in **F**, ventral; **G**, dorsal; and **H**, proximal views; a left tibiotarsus, IVPP V 755 in **I**, posterior view. **Abbreviations**: dc, dorsal cotyle; etd, extensor tendon process; ms, muscle scar; pe, posterior expansion; pf, pneumatic foramen; sw, swelling; tub, prominent tubercle; vc, ventral cotyle. Arrow indicates anterior in **D** and **E**. The lower left scale bar equals 10 mm and applies to **A**–**E**; the lower right scale bar equals 50 mm and applies to **F**–**I**.

sinensis (IVPP V 16047), the proximal portion of the expanded area is excavated into a lateral fossa (Wang et al., 2009, 2010). In pterodactyloids, e.g., *No. complicidens*, *H. tianshanensis*, the anhanguerian NMV P231549 and AODF 2297, and *Germanodactylus cristatus* (BSP 1892 IV 1), both the expanded area and lateral fossa are present, and additionally a distinct process is present proximimomedial to the lateral fossa (Fig. 6F, H; Pentland et al., 2022). This distinct process is called 'greater trochanter' (but see Lü et al., 2008: ch70), which is followed here. However, it should be noted that the bulged area rather than the distinct process is homologous with the structure with same name in other archosaurs, as a distinct process does not appear in basal pterosaurs, but the expanded area is universally present. The lesser trochanter is a tubercle or longitudinal scar on the anterolateral side of the proximal femoral shaft

(Fig. 6F–I). Novas (1996) hypothesized that the pterosaurian 'greater trochanter' (PGT) is homologous to the lesser trochanter of other ornithodirans (OLT). Hutchinson (2001a) followed this and that further suggested that the pterosaurian lesser trochanter (PLT) represents PIFI2 insertion. However, few evidence was provided to support this hypothesis.

Several clues inconsistent with the hypothesis of Novas (1996) and Hutchinson (2001a) are provided here that support homology between PLT and OLT. First, homologizing PGT and OLT is not parsimonious as previously suggested by Hutchinson (2001a). PGT is not universal to all pterosaurs but a tubercle on the anterior surface of proximal femur (PLT) is present with or without the PGT, e.g., *Quetzalcoatlus lawsoni* (with PGT) and *Raeticodactylus filisurensis* (without PGT) (Fig. 6I; Ezcurra et al., 2020; Andres and

Table 1
Measurements from IVPP V 746 and IVPP V 747. **Abbreviations**: AP, anteroposterior length; DV, dorsoventral length; ML, mediolateral length; PD, proximodistal length.

Element	Dimensions	Measurements (mm)
IVPP V 746, right femur	Proximal fragment length	49.35
	Middle fragment length	77.18
	Distal fragment length	41.50
	Shaft diameter at proximal breakage (AP & ML)	8.82 & 9.59
	'Greater trochanter' elevation	8.26
	Neck diameter (minimum & maximum)	5 & 7.2
	Neck length	10.36
	Distal end width	20.13
	Head diameter	11.8
IVPP V 746, right second wing phalanx	Proximal articular surface diameter (DV & AP)	8.18 & 16.34
	Proximal end diameter (DV & AP)	8.18 & 18.13
	Diameter at distal portion (DV & AP)	3.22 & 7.96
IVPP V 747, right first wing phalanx	Preserved length (From tip of extensor tendon process)	112.59
	Proximal end (DV & AP)	10.02 & 17.40
	Shaft diameter (DV & AP)	3.48 & 6.02
	Ventral pneumatic foramen diameter (AP & PD)	2.80 & 5.15
IVPP V 747, right tibiotarsus	Preserved length	45.90
	Distal diameter (AP & ML)	5.05 & 6.76
	Proximal diameter (AP & ML)	6.61 & 10.87
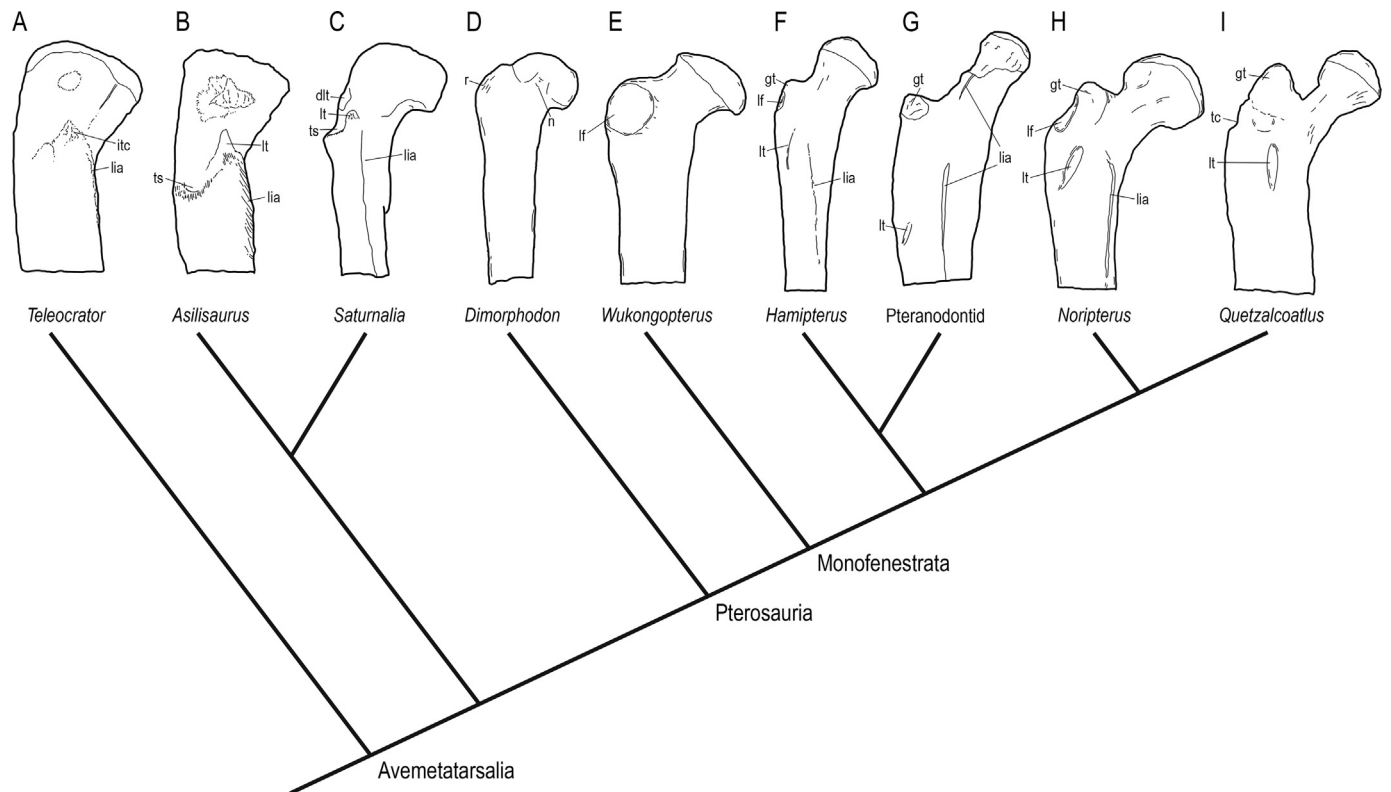
Fig. 6. Line drawings of proximal femora of pterosaurs and basal avemetatarsalians. **A–C**, right femora of *Teleocrator*, *Asilisaurus* and *Saturnalia* in anterior view, respectively (redrawn from Langer, 2003; Griffin and Nesbitt, 2016; Nesbitt et al., 2018); **D**, left femur of *Dimorphodon* in posterior view (redrawn from Sangster, 2021); **E**, right femur of *Wukongopterus lii* in anterolateral view; **F** and **G**, left femora (reversed) of *Hamipterus tianshanensis* and Pteranodontidae indet. (ZIN PH 66/43) in anterior view, respectively (redrawn from Averianov and Arkhangelsky, 2020); **H**, right femur of *Noripterus complicidens* in anterolateral view; **I**, right femur of *Quetzalcoatlus* cf. *northropi* in anterior view (redrawn from Andres and Langston, 2021). **Abbreviations**: gt, 'greater trochanter' (distinct process); itc, insertion for M. iliotrochantericus caudalis; lf, lateral fossa; lia, linea intermuscularis cranialis; lt, lesser trochanter; n, notch; r, rugose area; tc, 'trochanteric crest'; ts, trochanteric shelf.

Langston, 2021). Silesaurids, basal dinosaurs and at least some lagerpetids have OLT at a similar position as PLT (Fig. 6B, C; Nesbitt et al., 2009; Griffin and Nesbitt, 2016). Aphanosauria, the basal avemetatarsalian clade that forms the direct outgroup to Ornithodira, is also considered to have a muscle scar at a similar position as the lesser trochanter (Fig. 6A; Nesbitt et al., 2018). It is most parsimonious that the lesser trochanter arose only once in

avemetatarsalians. Homologizing the PGT and OLT will require at least two steps: a proximal shift of the OLT and the appearance of an additional tubercle, which is poorly supported by fossil evidence.

Secondly, the morphology of PLT and OLT are matched. Though the lesser trochanter often projects proximally in basal dinosaurs and is wing-like in theropods and ornithischians, in other basal avemetatarsalians it remains a tubercle or scar on the anterolateral

surface of the proximal shaft (Fig. 6A−C). This suggests that a tubercle-shaped lesser trochanter is the basal condition in ave-metatarsalians, and also in pterosaurs.

Third, an anterior ridge, if preserved, is closely associated with PLT in pterosaurs (Fig. 6F, H; Bertozzo et al., 2021). ZIN PH 66/43 is possibly an exception (Fig. 6G; Averianov and Arkhangelsky, 2020), but it most likely represents an autapomorphy. Similarly, an anterior ridge is always present in archosaurs. It is termed LIA and is a synapomorphy of archosaurs, as the division of M. femorotibialis of non-archosaur reptiles into M. femorotibialis internus (FMTI) and M. femorotibialis externus (FMTE) ancestrally in archosaurs (Hutchinson, 2001a). In extant archosaurs, LIA of birds originates from the anterior base of the trochanteric crest (Baumel and Witmer, 1993), which is formed by fusion of greater trochanter and lesser trochanter (Hutchinson, 2001a), whereas that of crocodiles originates more distally on the shaft, distal to the PIFI2 insertion (pers. obs.). In extinct avemetatarsalians, LIA always extends from the base of the lesser trochanter, e.g., *Teleocrator, Dromomeron gregorii, Asilisaurus*, basal dinosaurs (e.g., *Lesothosaurus, Herrerasaurus*, and *Saturnalia*) and pterosaurs (Fig. 6; Novas, 1994; Langer, 2003; Nesbitt et al., 2009; Maidment and Barrett, 2011; Griffin and Nesbitt, 2016; Nesbitt et al., 2018). The lesser trochanter provides insertion for part of iliofemoralis complex, and hence the conservative association between lesser trochanter and LIA in avemetatarsalians is an indication of retention of the contact relationship among FMTE, FMTI and iliofemoralis complex, which is present in extant archosaurs. If the OLT does shift proximally as in birds, the origination of LIA should also shift proximally to a similar position as seen in birds. It is not the case in pterosaurs, in which the LIA wraps around the lesser trochanter (Fig. 3A). Above all, the consistency of similarities between PLT and OLT suggests their homology.

3.2.2. M. puboischiofemoralis externus complex (PIFE) insertion

The presence of PIFE in pterosaurs is level I inference. Though the number of heads is equivocal (two heads in birds and three heads in crocodiles), it has no impact here as these heads have a common or closely associated insertion in extant archosaurs. PIFE1-3 insert on the greater trochanter (posterolateral to the head) in crocodiles; the correlates in birds (Mm. obturatorii lateralis et medialis) insert on the obturator ridge posterodistal to the trochanteric crest (Baumel and Witmer, 1993). The bulged area on the lateral aspect of the Laiyang femur is similar to the greater trochanter of crocodiles and other archosaurs, both in morphology and position. The lateral fossa is a modifed portion of the ancestral expanded area and is likely the main insertion for PIFE complex in the Laiyang femur. PIFE may also partially inserts on the expanded area distal to the lateral fossa, as the former is also slightly rugose. In *Quetzalcoatlus* the expanded area is further modified into a 'trochanteric crest', which may function the same as the lateral fossa in other pterosaurs (Andres and Langston, 2021). The PGT is a "novel" structure arising medial to the lateral fossa in pterodactyloids. In extant archosaurs this area does not insert any muscles. The function of PGT might be expanding the insertion area of PIFE and restricting the slipping of the tendon. In addition, the highly constricted femoral neck in pterosaurs means that acetabular ligaments could only insert onto the PGT, as these ligaments also inserts onto the trochanteric region in extant archosaurs (Tsai and Holliday, 2015).

3.2.3. Iliofemoralis complex (IF) insertion

Under the homology hypothesis of Rowe (1986), M. iliofemoralis (IF) of crocodiles is homologous to M. iliofemoralis externus (IFE) and M. iliotrochantericus caudalis (ITC) of birds. This means that the presence of this complex in pterosaurs is level I inference,

though the number of heads is equivocal. In crocodiles IF inserts on the anterolateral shaft; in birds. It was hypothesized that the lesser trochanter and trochanteric shelf in dinosaurs are osteological correlates for ITC and IFE respectively, and the insertion of IF shifts from the distal femoral shaft to the proximal shaft and splits into ITC and IFE on the lineage to birds (Rowe, 1986; Hutchinson, 2001a). The proximally shifted and splitted IF insertion was once thought to be present only in dinosauriforms. Recent discoveries and new hypothesis on avemetatarsalian phylogeny indicate that the lesser trochanter and trochanteric shelf were ancestrally present in bird-line archosaurs (Nesbitt et al., 2018; Ezcurra et al., 2020). As discussed above, the lesser trochanter of the Laiyang femur is homologous with that of other avemetatarsalians and provides insertion for ITC.

The corresponding structure of ornithodiran trochanteric shelf in pterosaurs remains to be solved. The trochanteric shelf is a horizontal structure that lies distolateral to the lesser trochanter. It may fuse with the lesser trochanter ontogenetically in ornithodirans (Griffin and Nesbitt, 2016). In pterosaurian femora other than the Laiyang femur, there is no tubercle, scar, or other structures distal to PLT that can be correlated with muscle attachment (Figs. 3, 6). This area is rather smooth in *No. complicidens*. The accessory tubercle in the Laiyang femur at this region also can not be homologous to the trochanteric shelf, as their morphologies do not match, i.e., the former is longitudinally aligned whereas the latter is horizontally aligned (Fig. 3A, G; Fig. 6B, C), and such change in morphology of the structure can not be traced in phylogeny. We hypothesize that the trochanteric shelf has reduced or fused with PLT in the early evolution of pterosaurs. IFE is either lost or fused with ITC and an iliofemoral complex is reconstructed here. The accessory tubercle of the Laiyang femur could represent an autapomorphic PIFI2 insertion. Intriguingly, the reduction of trochanteric shelf also occurred in dinosaurs. IFE is considered to be lost or fused with ITC in some birds (George and Berger, 1966; Rowe, 1986), and the two muscles are among the last to be separated in chick development (Romer, 1927). Ornithischians and sauropodomorphs also reduced or lost the trochanteric shelf (Maidment and Barrett, 2011). Therefore, the convergent loss of trochanteric shelf in pterosaurs is not unreasonable.

3.2.4. PIFI1 insertion

PIFI1 (= M. iliofemoralis internus in birds) is present in both birds and crocodiles, with a common insertion on the medial femoral shaft distal to the head (Romer, 1923; George and Berger, 1966). Bennett (2001a) considered the lesser trochanter to be the insertion for this muscle. This is incongruent with both the position of insertion for PIFI1 in extant archosaurs and the function of the lesser trochanter. The muscle scar for PIFI1 is rarely preserved in extinct archosaurs, but it develops into a ridge in the basal sauropodomorph *Saturnalia* (Langer, 2003). At a similar position as the PIFI1 insertion of extant archosaurs in the Laiyang femur, a longitudinal muscle scar is present and should be a candidate for the PIFI1 insertion (Figs. 2E, F, 3D). Additionally, the pattern of the scar orientation is posterodistal to anteroproximal, and is consistent with the origin of PIFI1 on the ventral and medial surfaces of the ilium body immediately anterior to the acetabulum (Frigot, 2018). This supports the identification of this muscle scar as PIFI1 insertion in pterosaurs.

3.2.5. PIFI2 insertion

The presence of PIFI2 is level I inference in extant archosaurs, yet the insertion is more equivocal. This muscle inserts on the anterolateral surface of the proximal femur in crocodiles, proximal to the IF insertion, whereas its homologues in birds (Mm. iliotrochanterici cranialis et medius) insert on the lateral surface of the

Table 2
Thigh muscles reconstructed in this article and the attachments of their homologues to femur in crocodiles and birds, mainly after Dilkes (2000) and Hutchinson (2002).

Thigh muscle names & abbreviations	Homologue in crocodiles	Homologue in birds	Insertion/origin in crocodiles	Insertion/origin in birds	Insertion/origin in IVPP V 746
Puboischiofemoralis internus 1 (PIFI1)	Puboischiofemoralis internus 1	Iliofemoralis internus	Medial to the fourth trochanter	Medial surface distal to the femoral head	Scar medial to the fourth trochanter
Puboischiofemoralis internus 2 (PIFI2)	Puboischiofemoralis internus 2	Iliotrochantericus cranialis & medialis	Proximolateral surface	Lateral surface distal to the trochanteric crest	Accessory tubercle
Iliofemoralis complex (IF)	Iliofemoralis	Iliofemoralis externus & liotrochantericus caudalis	Lateral surface of femoral shaft	Lateral surface distal to the trochanteric crest	Lesser trochanter
Femorotibiales internus (FMTI) et externus (FMTE)	Femorotibiales internus et externus	Femorotibiales lateralis et intermedius et medialis and other heads	On the femoral shaft, separated by intermuscular lines and adductor ridge	On the femoral shaft, separated by intermuscular lines and adductor ridge	On the femoral shaft, separated by intermuscular lines and adductor ridge
Caudofemoralis longus (CFL)	Caudofemoralis longus	Caudofemoralis pars pelvica	Fourth trochanter	Posterior femoral shaft	Fourth trochanter
Caudofemoralis brevis (CFB)	Caudofemoralis brevis	Caudofemoralis pars caudalis	Lateral to the fourth trochanter	Posterior femoral shaft	Not reconstructed here
Adductor femorales 1 et 2 (ADD1+2)	Adductor femorales 1 et 2	Puboischiofemorales medialis et lateralis	Adductor ridge	Adductor ridge	Lateral to the adductor ridge
Ischiotrochantericus (ISTR)	Ischiotrochantericus	Ischiofemoralis	Proximolateral femur, distal to the greater trochanter	Posterolateral surface distal to the trochanteric crest	Bulbous ridge
Puboischiofemoralis externus complex (PIFE)	Puboischiofemoralis externus 1-3	Obturatorii lateralis et medialis	Greater trochanter	Obturator ridge	Lateral fossa

trochanteric crest, distal to ITC and IFE insertion (Table 2; George and Berger, 1966). The different insertion of PIFI2 is seen in birds because on the line to birds the proximal femur is rotated medially, and the lesser trochanter, from the base of which arises the accessory trochanter for insertion of PIFI2, shifts proximally and fuses with the greater trochanter to form the trochanteric crest (Hutchinson, 2001a). As the proximal femur of pterosaurs retains the basal condition of directing anteromedially as in crocodiles, and that the PGT is not proximally shifted OLT, no features of pterosaurian femora will support a similar PIFI2 insertion as found in birds. Thus its insertion in pterosaurs should be more similar to that in crocodiles, i.e., on the anterolateral surface of the proximal femur.

However, another problem remains that, a change in the relative position of IF and PIFI2 is expected in bird-line archosaurs and this is also 'recapitulated' in chick development (Rowe, 1986), yet in which clade this change arose is not clear due to the lack of a consistent osteological correlate of PIFI2 in basal avemetatarsalians. This is also the case in pterosaurs. We tentatively reconstruct this muscle at the accessory tubercle ventral to the lesser trochanter in the Laiyang femur (Fig. 2F; 3G). This structure is not present in other pterosaurs but is similar in position to the accessory trochanter of tetanurans (Hutchinson, 2001a; Carrano and Hutchinson, 2002). Insertion of this muscle in other pterosaurs might occur in a similar area to the accessory tubercle in the Laiyang femur.

3.2.6. CFL insertion

The presence of CFB in pterosaurs is level I inference. The CFL insertion in archosaurs has a direct osteological correlate that is often called fourth trochanter, which is present in crocodiles but is absent in birds (Gatesy, 1990). Three hypotheses exist on the position of CFL insertion or fourth trochanter in pterosaurs: some pterosaur researchers consider the prominent tuberosity on the posterior ridges to be fourth trochanter (Kellner and Tomida, 2000; Bennett, 2001a; Andres and Langston, 2021); whereas others refer to the curved ridge or tuberosity on the posteromedial surface of the proximal shaft as fourth trochanter (McLain and Bakker, 2017; Bertozzo et al., 2021), which is at a similar position as reconstructed by Hutchinson (2001a); archosaur researchers think that the fourth trochanter is absent or reduced in pterosaurs (Gauthier, 1986; Nesbitt, 2011; Ezcurra et al., 2020). The first opinion probably rests on the basis that some birds have a CFL insertion on LIP, which is similar in position to the prominent tuberosity of pterosaurs. Further inspection on some specimens of *Pteranodon* sp. (YPM 1175, 2546) confirms that the "fourth trochanter" is actually surrounded by LIP and AR (Bennett, 2001a). Whether this is also the case in other pterosaurs reported to have a similarly positioned "fourth trochanter" remains to be confirmed. In crocodiles and basal archosaurs, the CFL insertion is proximal and medial to the LIP, and in basal avemetatarsalians, the insertion is even more proximally situated. Under the first hypothesis, the phylogenetic bracket requires an independent change of relative positions of CFL insertion and LIP in pterosaurs. The second hypothesis is accepted here, as it is more parsimonious with phylogeny (Fig. 2E). In addition, in pterosaurs the curved ridge often accompanies a depression at its medial side, which is also seen in many other archosaurs including crocodiles and basal avemetatarsalians (Gatesy, 1990; Nesbitt et al., 2018). Accepting such homology doesn't mean a conflict with the third hypothesis. Though the purported CFL insertion is a rather prominent structure in derived pterosaurs (Fig. 3D), it is rarely reported in basal pterosaurs. This is expected because such tuberosity or ridge is hardly preserved in crushed specimens, which is often the case in basal pterosaurs (Dalla Vecchia, 2013; Kellner, 2015). Nevertheless, the length of the fourth trochanter in pterosaurs has

been shortened compared with basal avemetatarsalians, although the gross morphology doesn't change much. In that sense, a "fourth trochanter" name for CFL insertion in pterosaurs is suitable. The term "internal trochanter" used by some authors to describe the same structure should be abandoned, for the fourth trochanter of archosauriforms is a derived state of internal trochanter of non-archosaurifom archosauromorphs and other reptiles (see discussions in Hutchinson, 2001a; Nesbitt, 2011), and the "internal trochanter" of pterosaurs actually represents a reduced fourth trochanter.

3.2.7. M. caudofemoralis brevis (CFB) insertion

The presence of CFB in pterosaurs is level I inference. Among extant archosaurs, this muscle inserts lateral to the fourth trochanter in crocodiles, whereas in birds the two bellies of M. caudofemoralis (when present), i.e., pars pelvica et caudalis, have a common or independent insertion on the shaft if present (George and Berger, 1966; McGowan, 1979). In basal avemetatarsalians, CFB often leaves a scar lateral to the fourth trochanter. However, in the Laiyang femur, *No. complicidens*, *D. weii*, and other pterosaurs no such scar is detected around the similar area. Whether this muscle is absent or merges with the CFL at the same insertion in pterosaurs cannot be determined. Although the origin of CFB was reconstructed on the ventral aspect of the postacetabular process of the ilium (Frigot, 2018), no osteological correlate was identified. It is not reconstructed here due to lack of osteological evidence. CFB may have been lost in the evolution of pterosaurs, as in many avian clades (George and Berger, 1966). The possibility also exists that CFB may have inserted between the fourth trochanter and the distal "tail" of the bulbous ridge in Pterosauria.

3.2.8. ISTR insertion

Whereas the presence of ISTR in pterosaurs is level I inference, its osteological correlate is not that clear. In extant archosaurs, this muscle inserts on the posterolateral surface of the proximal femur yet it lacks osteological correlates (Romer, 1923; McGowan, 1979). As ISTR belongs to the ventral mass of thigh muscles (Romer, 1927), it is expected to insert on the posterior or posterolateral femoral surface. In basal avemetatarsalians, no clear correlate of this muscle is found. The posterior trochanter of Eumaniraptora was interpreted as ISTR insertion (Hutchinson, 2001a). Similarly, the expansion distal to the greater trochanter in ornithischians was also interpreted as ISTR insertion (Maidment and Barrett, 2011). The bulbous ridge of the Laiyang femur and other pterosaurs is positioned at a similar location to the posterior trochanter and is reconstructed here to be insertion for ISTR (Fig. 2E), considering the conservative insertion of this muscle in archosaurs.

3.2.9. Ridges on the femoral shaft

On the shaft of the Laiyang femur, four ridges, i.e., one anterior ridge, one medial ridge, and two posterior ridges divide muscles (Fig. 2). The femoral shaft is covered by five muscles ancestrally in archosaurs (and retained in crocodiles): M. femorotibialis externus (FMTE), M. femorotibialis internus (FMTI), M. iliofemoralis (IF), and Mm. adductor femorales 1 et 2 (ADD) (Hutchinson, 2001a). FMTI is further divided into two heads in birds, i.e., Mm. femorotibiales intermedius (or medius) et medialis (or internus) in birds (George and Berger, 1966). As IF has shifted proximally in avemetatarsalians, at least four muscles are expected to be present on the femoral shaft of pterosaurs.

Three ridges, i.e., LIA, LIP, and AR, are ancestrally present in archosaurs to divide FMTE and FMTI, FMTE and ADD, ADD and FMTI respectively (Hutchinson, 2001a). Among extant archosaurs, LIA originates from the anterior base of trochanteric crest in birds, and it originates distally on the anterior femoral shaft in crocodiles

(Baumel and Witmer, 1993; Hutchinson, 2001a); it originates from the lesser trochanter in extinct avemetatarsalians. The anterior ridge of the Laiyang femur and other pterosaurs also originate from the lesser trochanter. It can be easily identified as LIA assuming that the conservative contact relationship among FMTE, FMTI and IF is retained in pterosaurs, as discussed above. LIP and AR originate distal to the fourth trochanter on the posterior femoral shaft in crocodiles; they originate immediately distal to the obturator ridge in birds (Baumel and Witmer, 1993). Among extinct avemetatarsalians, LIP originates from the trochanteric shelf in basal ornithodirans, e.g., *Dromomeron gregorii* and *Asilisaurus*, and basal saurischians (Langer, 2003; Nesbitt et al., 2009; Griffin and Nesbitt, 2016; Griffin, 2018); it originates from the expansion distal to the greater trochanter hypothesized to be ISTR insertion in ornithischians (Maidment and Barrett, 2011). A posteromedial division of LIP corresponding to AR is present in some dinosaurs, e.g., *Hypsilophodon* and *Saturnalia* (Galton, 1969; Langer, 2003), whereas this division is absent in many other avemetatarsalians. In the Laiyang femur, two posterior ridges originate distally on the shaft and seem to be dissociated with any other structure, except for some longitudinal faint scar proximal to their origination (Fig. 2A, E). These two posterior ridges are also observed in other pterosaurs, e.g., *No. complicidens*, *Pteranodon* sp., and '*Rhamphorhynchus*' *jessoni*, indicating that they are widely distributed (O'Sullivan, 2017; pers. obs.). They are most parsimoniously interpreted as LIP and AR in the aspect of their position. However, when compared with those of other avemetatarsalians, the origin of LIP loses association with the trochanteric shelf, which is hypothesized here to be lost or fused with the lesser trochanter in pterosaurs here. Moreover, a distinct AR is also not consistently present in avemetatarsalians, implying its presence is probably also variable across Pterosauria.

The presence of a medial ridge in the Laiyang femur is rather unexpected (Fig. 2A), as it is not present in extant archosaurs. It most probably divides the ancestral FMTI into an anterior part (FMTI1) and a posterior part (FMTI2; Fig. 2E, F). A similar division of the ancestral FMTI into two parts is also present in birds, rendering the reconstruction of this division as level II inference. A ridge at a similar position is also seen in some basal dinosaurs, e.g., *Hypsilophodon*, *Saturnalia* (Galton, 1969; Langer, 2003). It seems not universal to all avemetatarsalians or dinosaurs. In addition, this ridge is also seen in some other pterosaurs, e.g., *No. complicidens*, *Q. lawsoni*, *Q. northropi* and *Pteranodon* sp. (YPM 2546) (Andres and Langston, 2021). As the medial ridge is also scarcely reported in basal avemetatarsalians, it probably arises independently in different clades, and hence also the division of the FMTI.

4. Discussion

4.1. The attribution of IVPP V 746 femur and IVPP V 747 first wing phalanx

The Laiyang femur (IVPP V 746) and the first wing phalanx (IVPP V 747) preserve much anatomical information for comparison with other pterosaurs. The Laiyang femur certainly belongs to a pterodactyloid based on the constricted neck (present in pterodactyloids and derived non-pterodactyloids) and the elevated 'greater trochanter' (Wellnhofer et al., 1978). It bears many similarities to azhdarchoids and the characters supporting its affinity within this clade are listed and discussed separately below.

(1) Femoral neck, elongated and slender: Though the femoral necks are constricted in derived non-pterodactyloids and pterodactyloids, they are generally stout in archaeopterodactyloids, e.g., *Ardeadactylus* cf. *longicollum*, *Diocephalus kochi*, and *Germanodactylus cristatus*, dsungaripterids

and ornithocheiraean, e.g., *Hamipterus tianshanensis* and *Anhanguera piscator* (Fig. 5F, H; Plieninger, 1901; Young, 1964, 1973; Wellnhofer, 1970; Bakhurina, 1982; Lü et al., 2009; Rauhut et al., 2017; Augustin et al., 2021a; Bertozzo et al., 2021). This is in contrast to the condition in azhdarchoids, e.g., *Azhdarcho lancicollis* (ZIN PH 16/44), *Jidapterus edentus*, and *Sinopterus dongi*, and pteranodontians, e.g., *Pteranodon* sp., *Tethydraco regalis* and *Nyctosaurus gracilis*, that the femoral neck is slender and elongate (Fig. 5G, I; Williston, 1903; Bennett, 2001a; Averianov, 2010; Wu et al., 2017; Longrich et al., 2018; Zhang et al., 2019).

(2) Angle between the femoral neck and diaphysis, smaller than 145° but larger than 120°: The angle between the neck and diaphysis larger than 145° is a synapomorphy of pteranodontoids (Unwin, 2003; Andres, 2021), whereas this angle in the Laiyang femur is approximately 135°, higher than that of basal pterosaurs (e.g., 115° in *Seazzadactylus venieri*) but comparable with derived non-pterodactyloids and non-pteranodontoid pterodactyloids (Unwin, 2003; Dalla Vecchia, 2019).

(3) Shape of the 'greater trochanter', triangular and anteriorly curved: The morphology of the pterosaurian 'greater trochanter' has been compared previously in a phylogenetic context (Lü et al., 2008; Andres and Myers, 2012). The 'greater trochanter' is present in pterodactyloids and considered to be anteriorly curved in dsungaripterids and some azhdarchoids, e.g., *A. lancicollis*, *Chaoyangopterus zhangi* and *Tupuxuara leonardii* (Andres and Myers, 2012). However, our observation confirms that an anteriorly curved 'greater trochanter' is not restricted to these two clades and is more widely distributed. It is also present in *H. tianshanensis* and *G. cristatus*. In addition, the 'greater trochanter' of the Laiyang femur is also anteriorly curved, hence, relying solely on the curvature of the 'greater trochanter' is not sufficient for distinguishing it from either dsungaripterids, azhdarchoids, or other pterodactyloids (Andres and Myers, 2012).

The shape of 'greater trochanter' in anterior view might be a useful character, i.e., it is mediolaterally compressed in dsungaripterids (Fig. 6H), *H. tianshanensis*, two indetermined anhanguerian femora from Australia (NMV P231549; AODF 2297), and some archaeopterodactyloids, e.g., *G. cristatus* (Plieninger, 1901; Young, 1964; Wang et al., 2014a; Augustin et al., 2021a; Pentland et al., 2022), whereas it has a broader base and is triangular-shaped in azhdarchoids, e.g., *Caiuajara dobruskii*, *Tapejara wellnhoferi*, *Aralazhdarcho bostobensis*, *Az. lancicollis* (ZIN PH 16/44) and *Quetzalcoatlus lawsoni*, and pteranodontians, e.g., *Alcione elainus*, *Barbaridactylus grandis* and *Pteranodon* sp. (Fig. 6I; Averianov, 2007; Eck et al., 2011; Manzig et al., 2014; Andres and Langston, 2021). Though the main portion of the 'greater trochanter' is broken away in the Laiyang femur, its broad base shows similarity with pteranodontians and azhdarchoids (Fig. 3A, G). The preserved part also suggests that it is anteriorly curved, as in azhdarchoids yet different from pteranodontians, whose 'greater trochanter' directs proximally (Fig. 6G; Longrich et al., 2018; Averianov and Arkhangelsky, 2020). Although the 'greater trochanter' is also not anteriorly curved in the azhdarchid *Thanatosdrakon amaru*, this is more likely to represent its autapomorphy (Ortiz David et al., 2022).

(4) Proximal end of femur, pneumatic foramen, present: In pterodactyloids, a pneumatic foramen on the posterior aspect of the proximal end is present in azhdarchoids, e.g., *S. dongi*, *C. dobruskii*, *Az. lancicollis* (ZIN PH 16/44) and *Q. lawsoni*, pteranodontians, e.g., *Ny. gracilis*, *Alione elainus*, and *Pteranodon* sp., and *Istiodactylus latidens* (Williston, 1903; Hooley, 1913; Bennett, 2001b; Manzig et al., 2014;

Longrich et al., 2018; Zhang et al., 2019), whereas it is absent in dsungaripterids, e.g., *D. weii*, *No. complicidens* and the Tatal pterosaur, ornithocheiraeans, e.g., *An. piscator*, *Barbosania gracilirostris*, and *H. tianshanensis*, and archaeopterodactyloids, e.g., *Pterodactylus antiquus*, *Ardeadactylus* cf. *longicollum* (Young, 1964; Kellner and Tomida, 2000; Lü et al., 2009; Elgin and Frey, 2011; Wang et al., 2014a; Rauhut et al., 2017; Andres, 2021). The condition in istiodactiliforms other than *I. latidens* and boreopterids cannot be confirmed. A deep 'intertrochanteric fossa' with a pneumatic foramen is present in the Laiyang femur (Fig. 3E, F).

(5) Bulbous ridge, present: The bulbous ridge is a rugose tuberosity distal to the 'greater trochanter' on the posterior aspect of the proximal femoral shaft (Fig. 3D, J). It is present in azhdarchoids, e.g., *C. dobruskii*, *S. dongi*, and *Q. lawsoni* (Manzig et al., 2014; Zhang et al., 2019; Andres and Langston, 2021) but absent in dsungaripterids and pteranodontians, e.g., *Pteranodon* sp. and the indeterminate pteranodontid ZIN PH 66/43, and *An. piscator* (Kellner and Tomida, 2000; Bennett, 2001b; Averianov and Arkhangelsky, 2020).

(6) Curvature of the femoral shaft, mildly bowed anteriorly: Variations of femoral curvature among pterosaurs have long been noticed (Hooley, 1913). Although it was proposed that strongly bowed femur is a synapomorphy of Dsungaripteridae (Unwin, 2003; Fastnacht, 2005), this is not the case in at least one specimen of *No. complicidens* (IVPP V 4059), suggesting some variations affected by taphonomy. In *Q. lawsoni* and *Pteranodon* sp., the variation among orientations of different femoral specimens has also been recognized (Bennett, 2001a; Andres and Langston, 2021). Therefore, the curvature of femoral shaft in the aspect of both orientation and degree should be used with caution for taxonomic assignments. Besides this controversy, according to the coding in Andres (2021), femora of *Cryodrakon boreas*, *Q. lawsoni* and *Quetzalcoatlus northropi* are strongly bowed as in dsungaripterids. In addition, *Pterodaustro guinazui* also has a strongly bowed femur (Bonaparte, 1970; Codorniú et al., 2013), suggesting a wider distribution of this character in pterodactyloids. Pteranodontians share the derived trait in that their femora bow anteromedially (Longrich et al., 2018). Although this character has not been tested in phylogenetic analysis, its distribution among taxa proves useful in taxonomy (Bennett, 2001a; Longrich et al., 2018). The Laiyang femur is mildly bowed anteriorly, a trait widely distributed in pterodactyloids and possibly representing a basal condition of this clade.

(7) Mm. adductor femorales 1 et 2, proximally displaced: The area between LIP and AR provides insertion for ADD. The ADD insertion is close to the distal end and LIP reaches the margin of one of the distal condyles in *D. weii*, *No. complicidens*, and '*R*'. *jessoni* (NHMUK PV R 1755; O'Sullivan, 2017). The muscle scar proximal to the medial condyle in the nyctosaurids *Ny. gracilis* and *Alcione elainus* probably also corresponds to LIP (Williston, 1903; Longrich et al., 2018). The ADD insertion is proximally displaced in the Laiyang femur, *Az. lancicollis*, *Q. northropi* ("fourth trochanter" and accompanied groove in Andres and Langston, 2021), *An. piscator*, *H. tianshanensis*, *Pteranodon* sp. (YPM 1175, 2546), and the pteranodontian MGUAN-PA163 (possibly belongs to *Epapatelo otyikokolo*) (Fig. 2A, C; Kellner and Tomida, 2000; Averianov, 2010; Andres and Langston, 2021; Fernandes et al., 2022).

(8) Lateral condyle of the distal end, pulley-like: The morphology of the femoral condyles has received scant attention in pterosaurian taxonomy. In azhdarchoids and

dsungaripterids, the medial side of the medial condyle ("epicondyles" of Andres and Langston, 2021) develops into a distinct ridge (Andres, 2021). This is also the case in the Laiyang femur. Futhermore, the morphology of the lateral condyle is different in these two clades. In dsungaripterids, the lateral condyle tapers posterolaterally and does not bear a groove and bilateral ridges, as also seen in pteranodontoids, e.g., *An. piscator*, *H. tianshanensis*, *Pteranodon* sp. and the indetermined pteranodontid ZIN PH 66/43, and the thalassodromine *Tu. leonardii* (Bennett, 2001b; Veldmeijer, 2003; Kellner et al., 2016; Averianov and Arkhangelsky, 2020). A pulley-like lateral condyle is seen in *Az. lancicollis* (ZIN PH 20/44; Averianov, 2010), *C. dobruskii* and an indetermined azhdarchid MTM V 2010.99.1. from Hungary (Ősi et al., 2011; possibly belongs to *Bakonydraco galaczi*, a tapejarine according to Pêgas et al., 2021), which was first identified as a fourth metacarpal but considered by Averianov (2014) to be a distal fragment of a femur. The latter identification is followed here. Although most of the lateral condyle of the Laiyang femur was broken away, the presence of a medial ridge indicates it is also pulley-like (Fig. 4A, B).

The listed characters suggest that the Laiyang femur can be safely excluded from Dsungaripteridae (contra Young, 1964), as latter clade differs from the Laiyang femur in that the femoral neck is relatively stout, 'greater trochanter' is triangular-shaped, the proximal pneumatic foramen, bulbous ridge and medial ridge are absent, insertion for Mm. adductor femorales 1 et 2 is distally displaced and the lateral condyle is not pulley-like. Instead, the Laiyang femur can be assigned to Azhdarchoidea with confidence, yet further taxonomic assignment proves difficult. Azhdarchoidea is composed of three main clades, i.e., Tapejaridae, Chaoyangopteridae and Azhdarchidae (Pêgas et al., 2021). Tapejaridae is further composed of Thalassodrominae and Tapejarinae (Pêgas et al., 2021). At least one character distinguishes the Laiyang femur from the thalassodromine *Tu. leonardii*, i.e., a pulley-like lateral condyle, which is instead present in the tapejarine *C. dobruskii* and MTM V 2010.99.1. Tapejarine and chaoyangopterid femora are known from flattened or isolated specimens and are generally similar to the Laiyang femur. No specific character can be used for assignment of the Laiyang femur to these two clades.

Some well-preserved azhdarchid femora make detailed comparisons possible. The Laiyang femur differs from *Az. lancicollis* (ZIN PH 20/44) in that the latter has a deep intercondylar sulcus distally and a symmetrical distal end (Averianov, 2010). Whether the latter feature represents an autapomorphy of *Az. lancicollis* or synapomorphy of a more inclusive group is currently unknown. The Laiyang femur differs from *Th. amaru* in that the latter has a median ridge crossing the 'greater trochanter' and the 'greater trochanter' is not anteriorly curved (Ortiz David et al., 2022). It also differs from *Q. lawsoni* in the lack of a strongly bowed shaft and the 'trochanteric crest' (Andres and Langston, 2021). The 'trochanteric crest' is modified expanded area distal to the 'greater trochanter' on the lateral aspect of the femur and is not seen in other azhdarchoids. Lack of synapomorphies among azhdarchid femora precludes the assignment of the Laiyang femur to this group. Above all, the Laiyang femur is identified here as Azhdarchoidea indet. The individual represented by the femur is estimated to have a 2.2–2.9 m wingspan (using the method of Bennett, 2001b and the dataset of Andres and Langston, 2021).

The Laiyang first wing phalanx (IVPP V 747) represents a different taxon from the Laiyang femur, as these two elements both come from mature individuals and the sizes of which do not match. It can be confidently assigned to the non-dsungaripterid Ornithocheiroidea based on the presence of a proximal ventral pneumatic foramen

(Young, 1964; Bakhurina, 1982; Andres, 2021; Augustin et al., 2021b). Furthermore, its proximal end has a distinct posterior expansion, which is different from pteranodontoids, e.g., *Pteranodon* sp., *Ny. gracilis*, *Muzquizopteryx coahuilensis*, *Istiodactylus sinensis*, *Ikrandraco avatar*, *Boreopterus cuiae*, *H. tianshanensis* and *An. piscator*, whose posterior expansion is more gradual (Williston, 1903; Hooley, 1913; Kellner and Tomida, 2000; Bennett, 2001a; Lü and Ji, 2005; Andres and Ji, 2006; Frey et al., 2012; Wang et al., 2014a,b). It is further different from pteranodontids and lanceodontians in that the ETD of the latter two clades possesses a distinct proximal groove separating the ETD into two processes. In azhdarchoids, e.g., *Tu. leondardii*, *S. dongi*, *J. edentus* and *Az. lancicollis* (ZIN PH 36/44), dsungaripterids, and non-pteranodontid pteranodontians, e.g., *Alamodactylus byrdi*, *Muzquizopteryx coahuilensis* and *Ny. gracilis*, the proximal groove is not present or weakly developed, as in IVPP V 747 (Young, 1964, 1973; Kellner and Campos, 1988; Averianov, 2010; Andres and Myers, 2012; Kellner, 2013; Wu et al., 2017; Andres and Langston, 2021; Augustin et al., 2021a). However, at least one first wing phalanx of *Pteranodon* sp. (YPM 1164) shows the presence of a distinct posterior expansion and the absence of a proximal groove of ETD (Eaton, 1910). This suggests these characters are variable among individuals of the same taxon. Thus the Laiyang first wing phalanx is identified here as Ornithocheiroidea indet.

4.2. Comments on the pterosaurian humerus from the Doushan Formation

Pterosaur remains are very scarce in the Doushan Formation in Laiyang, Shandong Province, China. Apart from the materials described here (Young, 1958, 1964), only a fragmentary humerus PMOL-AP00018 has been reported (Zhou, 2010). PMOL-AP00018 preserves the deltopectoral crest (but missing its proximal and ventral tip) and most of the shaft. Zhou (2010) assigned the humerus to the Azhdarchidae based on the swollen and ventrally displaced terminal part of the deltopectoral crest. However, this character is also present in many other non-azhdarchid azhdarchoids, e.g., *S. dongi* (Zhou et al., 2022), *J. edentus* (Wu et al., 2017), an indetermined thalassodromine AMNH 22567 (Aires et al., 2014), and the archaeopterodactyloid *Forfexopterus jeholensis* (Zhou et al., 2020), which means that it cannot be considered as a synapomorphy of Azhdarchidae. Nevertheless, PMOL-AP00018 can be assigned to the Pterodactyloidea based on the elongated deltopectoral crest and straight shaft. It is further excluded from Pteranodontoidea based on the non-warped deltopectoral crest (Bennett, 1989; Padian and Smith, 1992). The distal margin of the deltopectoral crest is straight, distinct from the 'torted' morphology described in some azhdarchids (Padian and Smith, 1992; Andres and Langston, 2021). However, lack of synapomorphies of any pterodactyloid group in PMOL-AP00018 precludes further assignment. Therefore, it is identified here as Pterodactyloidea indet.

4.3. Comparison with former studies on pterosaurian thigh muscle reconstruction

Aside from this work, Hutchinson (2001a); Fastnacht (2005); Costa et al. (2013); Frigot (2018) also attempted to reconstruct hindlimb muscles in pterosaurs. Hutchinson (2001a) briefly discussed the femoral osteological correlates. Fastnacht (2005) and Costa et al. (2013) mainly focused on hindlimb biomechanics but did not provide osteological correlates for thigh muscles on the femur. The main difference between this work and Hutchinson's (2001a) is that the insertion of iliofemoralis complex is reconstructed differently as discussed above. In addition, Hutchinson (2001a: fig. 8) reconstructed ISTR on the anterior surface of the femur below the pterosaurian lesser trochanter. Whether this area is represented by scar or

tubercle is unclear. In the Laiyang femur this area is occupied by the accessory tubercle, whereas in other pterosaurs this area is rather smooth. ISTR is not likely insert on the anterior surface of femur in pterosaurs, as it belongs to the ventral mass of thigh muscles and also inserts on the posterolateral surface in extant archosaurs. ISTR originates from the medial side of the ischium and if it does insert on the position suggested by Hutchinson (2001a), it will turn direction abruptly at the lateral side of the femur close to its insertion, and this is functionally inefficient. Costa et al. (2013) generally followed Hutchinson (2001a) in the position of thigh muscle insertion. Fastnacht (2005) did not apply an EPB method and based the reconstruction mainly on birds. Fastnacht (2005) viewed iliotrochantericus muscle (three muscles in birds) as a whole, probably homologizing it with PIFI2 as in Romer (1927), which is in contrary to the homology hypothesis here (Rowe, 1986). M. iliotrochantericus was reconstructed to insert on the lateral fossa, as was also M. puboischiofemoralis, which according to its origin corresponds to PIFE here. M. iliofemoralis, as figured by Fastnacht (2005) originating on the ilium immediately above the acetabulum, apparently corresponds to IFE in birds. This muscle is considered to be lost or fused with ITC here.

Frigot (2018) focused on pelvic osteological correlates of hindlimb muscles in *Vectidraco daisymorrisae*, a purported azhdarchoid with partial pelvis and sacrum preserved. *Vectidraco* was recently recovered as a tapejarid pterosaur (Andres, 2021, = same as tapejarine in the phylogeny of Pêgas et al., 2021), and the Laiyang femur is identified here as an azhdarchoid. The pelvis of *V. daisymorrisae* might be good correlate for the Laiyang femur. Although direct comparison with the work of Frigot (2018) is impossible, some comments are made on the muscular origins discussed above.

A main difference with the muscular homology applied here in the reconstruction of Frigot (2018) lies in M. iliofemoralis. It was considered to originate on the ilium immediately posterior to the acetabulum, as in previous reconstructions (Fastnacht, 2005; Costa et al., 2013). This muscle complex is here considered to be composed of only ITC, and is more likely to originate on the preacetabular process, given a similar origin in birds (McGowan, 1979; Hutchinson, 2001b). On which surface of the process ITC originates is more equivocal, as it is currently unclear how the dorsoventrally flattened preacetabular process evolved from the ancestral archosaur state that is mediolaterally flattened (e.g., Hutchinson 2001b; Ezcurra et al., 2020). In previous reconstructions muscles were suspected to originate from the lateral margin (Costa et al., 2013; Frigot, 2018). However, the 90° difference from the ancestral state in pterosaurs might be explained by rotation. This process is probably detached from the sacrum and rotate medially, as is also the ilium body. If this is indeed the case, ITC most likely originates from the lateral portion of the dorsal surface of the preacetabular process, functioning mainly as a protractor and to a lesser extent a medial rotator and adductor. PIFI origin (PIFI1 and 2 were undifferentiated) was reconstructed on the "ventral iliac fossa" and the opposite side, and transverse processes of synsacrum (Frigot, 2018). The "ventral iliac fossa" is more likely to be the dorsal process of pubis as suggested by unfused specimens, e.g., *S. dongi* (SDUST-V1012) and *Ta. wellnhoferi* (SMNK PAL 1137) (Eck et al., 2011; Zhou et al., 2022). PIFI1 probably originates here and PIFI2 has a more anterior origin as reconstructed by Costa et al. (2013), e.g., on the ventral surface of preacetabular process. Hence the former may function mainly as a adductor and the latter as a protractor.

CFB origin was reconstructed on a small area of the ventral surface of the postacetabular process, largely due to absence of osteological correlate, which is often in the form of a fossa at a similar position in dinosaurs (Hutchinson, 2001b). No such fossa is present in the pterosaurian pelvis, and the area near where this fossa is expected is waisted, indicating either CFB is minor or originates from

sacrals or caudals as in crocodiles (Romer, 1923). The lack of a distinct insertion suggests that the former might be true.

PIFE origin was reconstructed on the lateral and medial surfaces of the pubis but not on the lateral surface of the ischium (Costa et al., 2013; Frigot, 2018). Instead, the anterior portion of the latter was entirely reconstructed as ADD origin. This is in contrast to the condition in crocodiles and lizards (Dilkes, 2000). PIFE and ADD mainly adduct the femur, which might be important in flapping flight, considering the parasagittal gait utilized by pterosaurs in terrestrial locomotion (Bennett, 1997). This might account for the retaining of the ischiopubic plate in pterosaurs, which is otherwise reduced or absent in archosaurs with a parasagittal posture (with lagerpetid as a possible exception) (Hutchinson, 2001b; Ezcurra et al., 2020). As the pterosaurian acetabular joint allows for wide range of motion, these two muscles might also help maintain posture and avoid collapse of the hindlimb during terrestrial locomotion.

5. Conclusions

The purported dsungaripterid remains from the Doushan Formation are redescribed. The most complete element, the IVPP V 746 femur, is assigned to Azhdarchoidea based on the combination of derived and plesiomorphic characters: a slender and elongated neck, angle between the neck and shaft smaller than 145° but larger than 120°, a triangular and anteriorly curved 'greater trochanter', a deep 'intertrochanteric fossa' with a pneumatic foramen, presence of a bulbous ridge, shaft mildly bowing anteriorly, presence of the medial ridge, proximally displaced Mm. adductor femorales 1 et 2 insertion and a pulley-like lateral condyle. Although the affinity of IVPP V 747 first wing phalanx cannot be determined to the rank of the femur, a dsungaripterid identity can be confidently excluded, and is here assigned to Ornithocheiroidea indet. Another pterosaurian humerus from the Doushan Formation was assigned by Zhou (2010) to Azhdarchidae, and cannot be determined beyond Pterodactyloidea indet.

Osteological correlates for thigh muscles on the femur are identified using the extant phylogenetic bracketing. The pterosaurian 'greater trochanter' is not homologous to the lesser trochanter of other ornithodirans, contrary to the previous hypotheses. Instead, it probably expands and restricts the insertion area of PIFE, and provides insertion for acetabular ligaments. FMTI is subdivided and ADD insertion is proximally displaced in some pterosaurs. Hip adductors might be involved in flapping flight and account for the retaining of the ischiopubic plate in pterosaurs.

References

Aires, A.S.S., Kellner, A.W.A., Müller, R.T., Da Silva, L.R., Pacheco, C.P., Dias-Da-Silva, S., 2014. New postcranial elements of the Thalassodrominae (Pterodactyloidea, Tapejaridae) from the Romualdo Formation (Aptian-Albian), Santana Group, Araripe Basin, Brazil. Palaeontology 57, 343−355.

Allen, V.R., Kilbourne, B.M., Hutchinson, J.R., 2021. The evolution of pelvic limb muscle moment arms in bird-line archosaurs. Science Advances 7, eabe2778.

Andres, B., 2021. Phylogenetic systematics of *Quetzalcoatlus* Lawson 1975 (Pterodactyloidea: Azhdarchoidea). Journal of Vertebrate Paleontology 41, 203–217.

Andres, B., Ji, Q., 2006. A new species of *Istiodactylus* (Pterosauria, Pterodactyloidea) from the Lower Cretaceous of Liaoning, China. Journal of Vertebrate Paleontology 26, 70–78.

Andres, B., Langston, W., 2021. Morphology and taxonomy of *Quetzalcoatlus* Lawson 1975 (Pterodactyloidea: Azhdarchoidea). Journal of Vertebrate Paleontology 41, 46–202.

Andres, B., Myers, T.S., 2012. Lone star pterosaurs. Earth and Environmental Science Transactions of the Royal Society of Edinburgh 103, 383–398.

Augustin, F.J., Matzke, A.T., Maisch, M.W., Csiki-Sava, Z., 2021a. Pterosaur remains from the Lower Cretaceous Lianmuxin Formation (upper Tugulu Group) of the southern Junggar Basin (NW China). Historical Biology 34, 312–321.

Augustin, F.J., Matzke, A.T., Maisch, M.W., Pfretzschner, H.-U., 2021b. New information on *Lonchognathosaurus* (Pterosauria: Dsungaripteridae) from the Lower Cretaceous of the southern Junggar Basin (NW China). Cretaceous Research 124, 104808.

Averianov, A.O., 2014. Review of taxonomy, geographic distribution, and paleoenvironments of Azhdarchidae (Pterosauria). ZooKeys 432, 1–107.

Averianov, A.O., 2007. New records of azhdarchids (Pterosauria, Azhdarchidae) from the Late Cretaceous of Russia, Kazakhstan, and Central Asia. Paleontological Journal 41, 189–197.

Averianov, A.O., 2010. The osteology of *Azhdarcho lancicollis* Nessov, 1984 (Pterosauria, Azhdarchidae) from the late Cretaceous of Uzbekistan. Proceedings of the Zoological Institute RAS 314, 264–317.

Averianov, A.O., Arkhangelsky, M.S., 2020. A large pteranodontid pterosaur from the Late Cretaceous of Eastern Europe. Geological Magazine 158, 1143–1155.

Bakhurina, N., 1982. A pterodactyl from the Lower Cretaceous of Mongolia. Paleontological Journal 4, 104–108.

Barrett, P.M., Butler, R.J., Edwards, N.P., Milner, A.R., 2008. Pterosaur distribution in time and space: an atlas. Zitteliana B28, 61–107.

Baumel, J.J., Witmer, L.M., 1993. Osteologia. In: Baumel, J.J. (Ed.), Handbook of Avian Anatomy: Nomina Anatomica Avium, second ed. Nuttall Ornithological Club, Cambridge, Massachusetts, pp. 45–132.

Benjamin, M., Kumai, T., Milz, S., Boszczyk, B.M., Boszczyk, A.A., Ralphs, J.R., 2002. The skeletal attachment of tendons—tendon 'entheses'. Comparative Biochemistry and Physiology Part A: Molecular & Integrative Physiology 133, 931–945.

Bennett, S.C., 1989. A pteranodontid pterosaur from the Early Cretaceous of Peru, with comments on the relationships of Cretaceous pterosaurs. Journal of Paleontology 63, 669–677.

Bennett, S.C., 1993. The ontogeny of *Pteranodon* and other pterosaurs. Paleobiology 19, 92–106.

Bennett, S.C., 1997. Terrestrial locomotion of pterosaurs: a reconstruction based on Pteraichnus trackways. Journal of Vertebrate Paleontology 17, 104–113.

Bennett, S.C., 2001a. The osteology and functional morphology of the Late Cretaceous pterosaur *Pteranodon* Part I. General description of osteology. Palaeontographica Abteilung A 260, 1–112.

Bennett, S.C., 2001b. The osteology and functional morphology of the Late Cretaceous pterosaur *Pteranodon* Part II. Size and functional morphology. Palaeontographica Abteilung A 260, 113–153.

Bertozzo, F., Camilo da Silva, B., Martill, D.M., Vorderwuelbecke, E., Aureliano, T., Schouten, R., Aquino, P., 2021. A large pterosaur femur from the Kimmeridgian, Upper Jurassic of Lusitanian Basin, Portugal. Acta Palaeontologica Polonica 66, 815–825.

Bonaparte, J., 1970. *Pterodaustro guiñazui* gen. et. sp. nov. Pterosaurio de la Formación Lagarcito, Provincia de San Luis, Argentina y su significado en la geología regional (Pterodactylidae). Acta Geológica Lilloana 10, 207–226.

Carrano, M.T., Hutchinson, J.R., 2002. Pelvic and hindlimb musculature of *Tyrannosaurus rex* (Dinosauria: Theropoda). Journal of Morphology 253, 207–228.

Codorniú, L., Chiappe, L.M., Cid, F.D., 2013. First occurrence of stomach stones in pterosaurs. Journal of Vertebrate Paleontology 33, 647–654.

Costa, F.R., Rocha-Barbosa, O., Kellner, A.W.A., 2013. A biomechanical approach on the optimal stance of *Anhanguera piscator* (Pterodactyloidea) and its implications for pterosaur gait on land. Historical Biology 26, 582–590.

Currey, J.D., Alexander, R.M., 1985. The thickness of the walls of tubular bones. Journal of Zoology 206, 453–468.

Dalla Vecchia, F.M., 2013. Triassic pterosaurs. Geological Society, London, Special Publications 379, 119–155.

Dalla Vecchia, F.M., 2019. *Seazzadactylus venieri* gen. et sp. nov., a new pterosaur (Diapsida: Pterosauria) from the Upper Triassic (Norian) of northeastern Italy. PeerJ 7, e7363.

Dilkes, D.W., 2000. Appendicular myology of the hadrosaurian dinosaur *Maiasaura peeblesorum* from the Late Cretaceous (Campanian) of Montana. Earth and Environmental Science Transactions of the Royal Society of Edinburgh 90, 87–125.

Eaton, G.F., 1910. Osteology of *Pteranodon*. Memoirs of the Connecticut Academy of Arts of Sciences 2, 1–38.

Eck, K., Elgin, R.A., Frey, E., 2011. On the osteology of *Tapejara wellnhoferi* Kellner 1989 and the first occurrence of a multiple specimen assemblage from the Santana Formation, Araripe Basin, NE-Brazil. Swiss Journal of Palaeontology 130, 277–296.

Elgin, R.A., Frey, E., 2011. A new ornithocheirid, *Barbosania gracilirostris* gen. et sp. nov. (Pterosauria, Pterodactyloidea) from the Santana Formation (Cretaceous) of NE Brazil. Swiss Journal of Palaeontology 130, 259–275.

Ezcurra, M.D., Nesbitt, S.J., Bronzati, M., Dalla Vecchia, F.M., Agnolin, F.L., Benson, R.B.J., Brisson Egli, F., Cabreira, S.F., Evers, S.W., Gentil, A.R., Irmis, R.B., Martinelli, A.G., Novas, F.E., Roberto da Silva, L., Smith, N.D., Stocker, M.R., Turner, A.H., Langer, M.C., 2020. Enigmatic dinosaur precursors bridge the gap to the origin of Pterosauria. Nature 588, 445–449.

Fastnacht, M., 2005. The first dsungaripterid pterosaur from the Kimmeridgian of Germany and the biomechanics of pterosaur long bones. Acta Palaeontologica Polonica 50, 273–288.

Fernandes, A.E., Mateus, O., Andres, B., Polcyn, M.J., Schulp, A.S., Gonçalves, A.O., Jacobs, L.L., 2022. Pterosaurs from the Late Cretaceous of Angola. Diversity 14, 741–768.

Frey, E., Elgin, R.A., Stinnesbeck, W., Padilla-Gutiérrez, J.M., Ifrim, C., Giersch, S., González-González, A.H., 2012. A new specimen of nyctosaurid pterosaur, cf. *Muzquizopteryx* sp. from the Late Cretaceous of northeast Mexico. Revista Mexicana de Ciencias Geológicas 29, 131–139.

Frey, E., Martill, D.M., 1998. Late ontogenetic fusion of the processus tendinis extensoris in Cretaceous pterosaurs from Brazil. Neues Jahrbuch für Geologie und Paläontologie - Monatshefte 10, 587–594.

Frigot, R.A., 2018. Pelvic musculature of *Vectidraco daisymorrisae* and consequences for pterosaur locomotion. Geological Society, London, Special Publications 455, 45–55.

Galton, P.M., 1969. The pelvic musculature of the dinosaur *Hypsilophodon* (Reptilia: Ornithischia). Postilla 131, 1–64.

Gatesy, S.M., 1990. Caudofemoral musculature and the evolution of theropod locomotion. Paleobiology 16, 170–186.

Gauthier, J., 1986. Saurischian monophyly and the origin of birds. Memoirs of the California Academy of Sciences 8, 1–55.

George, J.C., Berger, A.J., 1966. Avian Myology. Academic Press, New York.

Griffin, B., Martin-Silverstone, E., Demuth, O., Pêgas, R., Palmer, C., Rayfield, E., 2022. Constraining pterosaur launch: range of motion in the pectoral and pelvic girdles of a medium-sized ornithocheiraean pterosaur. Biological Journal of the Linnean Society 137, 250–266.

Griffin, C.T., 2018. Developmental patterns and variation among early theropods. Journal of Anatomy 232, 604–640.

Griffin, C.T., Nesbitt, S.J., 2016. The femoral ontogeny and long bone histology of the Middle Triassic (?late Anisian) dinosauriform *Asilisaurus kongwe* and implications for the growth of early dinosaurs. Journal of Vertebrate Paleontology 36, e1111224.

Hooley, R.W., 1913. On the skeleton of *Ornithodesmus latidens*; an ornithosaur from the Wealden Shales of Atherfield (Isle of Wight). Quarterly Journal of the Geological Society 69, 372–422.

Hu, C., Cheng, Z., Pang, Q., Fang, X., 2001. Shantungosaurus giganteus. Geological Publishing House, Beijing, p. 139.

Hutchinson, J.R., 2001a. The evolution of femoral osteology and soft tissues on the line to extant birds (Neornithes). Zoological Journal of the Linnean Society 131, 169–197.

Hutchinson, J.R., 2001b. The evolution of pelvic osteology and soft tissues on the line to extant birds (Neornithes). Zoological Journal of the Linnean Society 131, 123–168.

Hutchinson, J.R., 2002. The evolution of hindlimb tendons and muscles on the line to crown-group birds. Comparative Biochemistry and Physiology Part A: Molecular & Integrative Physiology 133, 1051–1086.

Kellner, A.W.A., 2015. Comments on Triassic pterosaurs with discussion about ontogeny and description of new taxa. Anais da Academia Brasileira de Ciências 87, 669–689.

Kellner, A.W.A., Tomida, Y., 2000. Description of a new species of Anhangueridae (Pterodactyloidea) with comments on the pterosaur fauna from the Santana Formation (Aptian-Albian), northeastern Brazil. National Science Museum Monographs 17, 1–137.

Kellner, A.W.A., 2013. A new unusual tapejarid (Pterosauria, Pterodactyloidea) from the Early Cretaceous Romualdo Formation, Araripe Basin, Brazil. Earth and Environmental Science Transactions of the Royal Society of Edinburgh 103, 409–421.

Kellner, A.W.A., Campos, D.A., 1988. Sobre um novo pterossauro com crista sagital da Bacia do Araripe, Cretáceo Inferior do Nordeste do Brasil. Anais da Academia Brasileira de Ciências 60, 459–469.

Kellner, A.W.A., Costa, F.R., Wang, X., Cheng, X., 2016. Redescription of the first pterosaur remains from Japan: the largest flying reptile from Asia. Historical Biology 28, 304–309.

Langer, M.C., 2003. The pelvic and hind limb anatomy of the stem-sauropodomorph *Saturnalia tupiniquim* (Late Triassic, Brazil). PaleoBios 23, 1–39.

Longrich, N.R., Martill, D.M., Andres, B., 2018. Late Maastrichtian pterosaurs from North Africa and mass extinction of Pterosauria at the Cretaceous-Paleogene boundary. PLoS Biology 16, e2001663.

Lü, J., Azuma, Y., Dong, Z., Barsbold, R., Kobayashi, Y., Lee, Y.-N., 2009. New material of dsungaripterid pterosaurs (Pterosauria: Pterodactyloidea) from western Mongolia and its palaeoecological implications. Geological Magazine 146, 690–700.

Lü, J., Ji, Q., 2005. A new ornithocheirid from the Early Cretaceous of Liaoning Province, China. Acta Geologica Sinica-English Edition 79, 157–163.

Lü, J., Unwin, D.M., Xu, L., Zhang, X., 2008. A new azhdarchoid pterosaur from the Lower Cretaceous of China and its implications for pterosaur phylogeny and evolution. Naturwissenschaften 95, 891–897.

Maidment, S.C.R., Barrett, P.M., 2011. The locomotor musculature of basal ornithischian dinosaurs. Journal of Vertebrate Paleontology 31, 1265–1291.

Manzig, P.C., Kellner, A.W.A., Weinschutz, L.C., Fragoso, C.E., Vega, C.S., Guimaraes, G.B., Godoy, L.C., Liccardo, A., Ricetti, J.H., de Moura, C.C., 2014. Discovery of a rare pterosaur bone bed in a cretaceous desert with insights on ontogeny and behavior of flying reptiles. PLoS One 9, e100005.

McGowan, C., 1979. The hind limb musculature of the brown kiwi, *Apteryx australis mantelli*. Journal of Morphology 160, 33–73.

McLain, M.A., Bakker, R.T., 2017. Pterosaur material from the uppermost Jurassic of the uppermost Morrison Formation, Breakfast Bench Facies, Como Bluff, Wyoming, including a pterosaur with pneumatized femora. Geological Society, London, Special Publications 455, 105–124.

Nesbitt, S.J., 2011. The Early Evolution of Archosaurs: Relationships and the Origin of Major Clades. Bulletin of the American Museum of Natural History 352, 1–292.

Nesbitt, S.J., Butler, R.J., Ezcurra, M.D., Charig, A.J., Barrett, P.M., 2018. The anatomy of *Teleocrater Rhadinus*, an early avemetatarsalian from the lower portion of the Lifua Member of the Manda Beds (Middle Triassic). Journal of Vertebrate Paleontology 37, 142–177.

Nesbitt, S.J., Irmis, R.B., Parker, W.G., Smith, N.D., Turner, A.H., Rowe, T., 2009. Hindlimb osteology and distribution of basal dinosauromorphs from the Late Triassic of North America. Journal of Vertebrate Paleontology 29, 498–516.

Novas, F.E., 1994. New information on the systematics and postcranial skeleton of *Herrerasaurus ischigualastensis* (Theropoda: Herrerasauridae) from the Ischigualasto Formation (Upper Triassic) of Argentina. Journal of Vertebrate Paleontology 13, 400–423.

Novas, F.E., 1996. Dinosaur monophyly. Journal of Vertebrate Paleontology 16, 723–741.

O'Sullivan, M., 2017. The pterosaur assemblage of the Oxford Clay Formation (Jurassic, Callovian–Oxfordian) from the UK. Geological Society, London, Special Publications 455, 171–180.

Ortiz David, L.D., González Riga, B.J., Kellner, A.W.A., 2022. *Thanatosdrakon amaru*, gen. et sp. nov., a giant azhdarchid pterosaur from the upper Cretaceous of Argentina. Cretaceous Research 137, 105228.

Ősi, A., Buffetaut, E., Prondvai, E., 2011. New pterosaurian remains from the Late Cretaceous (Santonian) of Hungary (Iharkút, Csehbánya Formation). Cretaceous Research 32, 456–463.

Padian, K., 1983. A functional analysis of flying and walking in pterosaurs. Paleobiology 9, 218–239.

Padian, K., 2008. The Early Jurassic pterosaur *Campylognathoides* Strand, 1928. Special Papers in Palaeontology 80, 65–107.

Padian, K., Smith, M., 1992. New light on Late Cretaceous pterosaur material from Montana. Journal of Vertebrate Paleontology 12, 87–92.

Pêgas, R.V., Holgado, B., Ortiz David, L.D., Baiano, M.A., Costa, F.R., 2021. On the pterosaur *Aerotitan sudamericanus* (Neuquén Basin, Upper Cretaceous of Argentina), with comments on azhdarchoid phylogeny and jaw anatomy. Cretaceous Research 129, 104998.

Pentland, A.H., Poropat, S.F., White, M.A., Rigby, S.L., Vickers-Rich, P., Rich, T.H., Elliott, D.A., 2022. New anhanguerian pterosaur remains from the Lower Cretaceous of Queensland, Australia. Alcheringa: An Australasian Journal of Palaeontology 46, 188–197.

Plieninger, F., 1901. Beiträge zur kenntniss der flugsaurier. Palaeontographica 48, 65–90.

Rauhut, O.W., López-Arbarello, A., Röper, M., Rothgaenger, M., 2017. Vertebrate fossils from the Kimmeridgian of Brunn: the oldest fauna from the Solnhofen Archipelago (Late Jurassic, Bavaria, Germany). Zitteliana 89, 305–329.

Romer, A.S., 1923. Crocodilian pelvic muscles and their avian and reptilian homologues. Bulletin of the American Museum of Natural History 48, 533–552.

Romer, A.S., 1927. The development of the thigh musculature of the chick. Journal of Morphology 43, 347–385.

Rowe, T., 1986. Homology and evolution of the deep dorsal thigh musculature in birds and other reptilia. Journal of Morphology 189, 327–346.

Sangster, S., 2021. The osteology of *Dimorphodon macronyx*, a non-pterodactyloid pterosaur from the Lower Jurassic of Dorset, England. Monographs of the Palaeontographical Society 175, 1–48.

Tsai, H.P., Holliday, C.M., 2015. Articular soft tissue anatomy of the archosaur hip joint: Structural homology and functional implications. Journal of Morphology 276, 601–630.

Unwin, D.M., 2003. On the phylogeny and evolutionary history of pterosaurs. Geological Society, London, Special Publications 217, 139–190.

Unwin, D.M., Heinrich, W.-D., 1999. On a pterosaur jaw from the Upper Jurassic of Tendaguru (Tanzania). Mitteilungen aus dem Museum für Naturkunde in Berlin. Geowissenschaftlichen Reihe 2, 121–134.

Upchurch, P., Andres, B., Butler, R.J., Barrett, P.M., 2015. An analysis of pterosaurian biogeography: implications for the evolutionary history and fossil record quality of the first flying vertebrates. Historical Biology 27, 697–717.

Veldmeijer, A.J., 2003. Description of *Coloborhynchus spielbergi* sp. nov.(Pterodactyloidea) from the Albian (Lower Cretaceous) of Brazil. Scripta Geologica 125, e139.

Wang, J., Zhou, C., Jourdan, F., Chang, S., 2022. Jehol fossils from the Jiaolai Basin of Shandong, North China: review and new perspectives. Geological Society, London, Special Publications 521, 209–223.

Wang, X., Kellner, A.W.A., Jiang, S., Cheng, X., Meng, X., Rodrigues, T., 2010. New long-tailed pterosaurs (Wukongopteridae) from western Liaoning, China. Anais da Academia Brasileira de Ciências 82, 1045–1062.

Wang, X., Kellner, A.W.A., Jiang, S., Meng, X., 2009. An unusual long-tailed pterosaur with elongated neck from western Liaoning of China. Anais da Academia Brasileira de Ciências 81, 793–812.

Wang, X., Kellner, A.W.A., Zhou, Z., Campos Dde, A., 2005. Pterosaur diversity and faunal turnover in Cretaceous terrestrial ecosystems in China. Nature 437, 875–879.

Wang, X., Kellner, A.W.A., Jiang, S., Wang, Q., Ma, Y., Paidoula, Y., Cheng, X., Rodrigues, T., Meng, X., Zhang, J., Li, N., Zhou, Z., 2014a. Sexually dimorphic tridimensionally preserved pterosaurs and their eggs from China. Current Biology 24, 1323–1330.

Wang, X., Rodrigues, T., Jiang, S., Cheng, X., Kellner, A.W.A., 2014b. An Early Cretaceous pterosaur with an unusual mandibular crest from China and a potential novel feeding strategy. Scientific Reports 4, 6329.

Wellnhofer, P., 1970. Die Pterodactyloidea (Pterosauria) der Oberjura-Plattenkalke Suddentschlands, Bayer. Bayerische Akademie der Wissenschaften, Mathematisch-Wissenschaftlichen Klasse, Abhandlungen 141, 1–133.

Wellnhofer, P., 1991. The Illustrated Encyclopedia of Pterosaurs. Salamander Books, London, p. 192.

Wellnhofer, P., Appleby, R.M., Kuhn, O., 1978. Handbuch der Paläoherpetologie: Pterosauria. Gustav Fisher, Stuggart, p. 82.

Williston, S.W., 1903. On the osteology of *Nyctosaurus* (*Nyctodactylus*), with notes on American pterosaurs. Field Columbian Museum Publications, Geological Series 2, 125–163.

Witmer, L.M., 1995. The extant phylogenetic bracket and the importance of reconstructing soft tissues in fossils. In: Thomason, J. (Ed.), Functional Morphology in Vertebrate Paleontology. Cambridge University Press, Cambridge, pp. 19–33.

Wu, W., Zhou, C., Andres, B., 2017. The toothless pterosaur *Jidapterus edentus* (Pterodactyloidea: Azhdarchoidea) from the Early Cretaceous Jehol Biota and its paleoecological implications. PLoS One 12, e0185486.

Xu, X., Zhou, Z., Sullivan, C., Wang, Y., Ren, D., 2016. An updated review of the Middle-Late Jurassic Yanliao Biota: chronology, taphonomy, paleontology and paleoecology. Acta Geologica Sinica-English Edition 90, 2229–2243.

Xu, Y., Jiang, S., Wang, X., 2022. A new istiodactylid pterosaur, *Lingyuanopterus camposi* gen. et sp. nov., from the Jiufotang Formation of western Liaoning, China. PeerJ 10, e13819.

Young, C.C., 1958. The dinosaurian remains of Laiyang, Shantung. Palaeontologica Sinica New Series C 16, 1–138.

Young, C.C., 1964. On a new pterosaurian from Sinkiang, China. Vertebrata PalAsiatica 8, 221–255.

Young, C.C., 1973. Pterosaurs from Wuerho, Reports of Paleontological Expedition to Sinkiang (II): Pterosaurian Fauna from Wuerho, Sinkiang. Science Press, Beijing, pp. 18–35.

Zhang, X., Jiang, S., Cheng, X., Wang, X., 2019. New material of *Sinopterus* (Pterosauria, Tapejaridae) from the Early Cretaceous Jehol Biota of China. Anais da Academia Brasileira de Ciências 91, e20180756.

Zhou, C., 2010. A possible azhdarchid pterosaur from the Lower Cretaceous Qingshan Group of Laiyang, Shandong, China. Journal of Vertebrate Paleontology 30, 1743–1746.

Zhou, C., Wang, J., Zhu, Z., 2020. A new wing skeleton of *Forfexopterus* (Pterosauria: Ctenochasmatidae) from the Early Cretaceous Jehol Biota reveals a developmental variation. Fossil Record 23, 191–196.

Zhou, C., Niu, T., Yu, D., 2022a. New data on the postcranial skeleton of the tapejarid *Sinopterus* from the Early Cretaceous Jehol Biota. Historical Biology 35, 356–363.

Zhou, C., Yu, D., Zhu, Z., Andres, B., 2022b. A new wing skeleton of the Jehol tapejarid *Sinopterus* and its implications for ontogeny and paleoecology of the Tapejaridae. Scientific Reports 12, 10159.